



Article submitted to journal

Subject Areas:

Physics, Biology, Chemistry

Keywords:

quantum, rate equation, golden rule, enzymes, olfaction, photosynthesis, magnetodetection

Author for correspondence:

Jennifer C. Brookes

e-mail: j.brookes@ucl.ac.uk

Quantum effects in biology: golden rule in enzymes, olfaction, photosynthesis and magnetodetection

Jennifer C. Brookes ¹

¹London Centre for Nanotechnology, University College London, 17-19 Gordon Street, London, UK, WC1E 6BT

Despite certain quantum concepts, such as superpositioned states, entanglement; ‘spooky action at a distance’ and tunneling through insulating walls, being somewhat counter-intuitive, they are no doubt extremely useful constructs in theoretical and experimental physics. More uncertain, however, is whether or not these concepts are fundamental to biology and living processes. Of course, at the fundamental level all things are quantum, because all things are built from the quantized states and rules that govern atoms. But when does the quantum mechanical toolkit become the best tool for the job? This review looks at four areas of “quantum effects in biology”. These are biosystems that are very diverse in detail but possess some commonality. They are all i) *effects* in biology: rates of a signal (or information) that can be calculated from a form of the “golden rule” and ii) they are all protein-pigment (or ligand) complex systems. It is shown, beginning with the rate equation, that all these systems may contain some degree of *quantum* effect, and where experimental evidence is available, it will be explored how the quantum analysis aids understanding of the process is explored.

1. Introduction

Four living processes are considered in this review: a reaction mechanism (enzyme catalysis), a sensory signal (olfaction), the transfer of energy (photosynthesis) and the encoding of information (magnetodetection). Though diverse areas, they have at least two common threads i) they are biosystems that may be understood in terms of a *rate* ii) and they are all biosystems consisting of a pigment (or pigment-like molecule, such as a ligand/odorant/flavin) in a protein environment. Examining the rate equation, based on Fermi's golden rule, will allow us to consider "quantum effects" and, surprisingly, it will be seen that the protein environment of these systems does not camouflage or collapse any state, but, conversely seems to not only *enable* the said rate, but to further- to *enhance*- it. The ways in which the full system is treated involves various degrees of "quantumness" and we shall see briefly how this is done in the four systems that follow. Firstly it is shown that the remarkably fast reaction rates of enzymes are accelerated by the tunneling phenomena. Secondly it is conjectured that the signalling in olfaction is also a tunneling effect, enabled by the presence of an odorant with a signature quantum mechanical vibration (its smell!). Thirdly it is seen that the superposition of excited states upon light excitation in photosynthesis supports long-lived coherent states that explain the efficiency of energy transfer. Fourthly, and finally, magnetoreception is briefly examined, where it may be seen that entangled states encode the angle of magnetic field lines, perceived in animals as differences in reaction rates. Thus, the common "quantum effect" hallmarks of tunneling, wave superposition /coherence, and the "spooky" entanglement phenomena are all represented. Where available, this review is written around experimental evidence and theory is described in order to explain/ predict the quantum effects. Whether any quantum theorizing illuminates and explains a biological effect is then briefly discussed in the conclusions with a final mention of the role of the environment and what remains as future work and challenges in the field.

(a) Rate equation

Be it a charge or energy transfer (or both) the systems discussed below share one commonality: a transition from one state to another, and the rate of the transition can be analysed with the rate equation, or the "golden rule":

$$rate(D \rightarrow A) = \frac{2\pi}{\hbar} |H_{DA}|^2 \rho, \quad (1.1)$$

where the rate describes a transition from D (donor, initial state, or reactant) to A (acceptor, final state, or product), where ρ is the density of states that can accept the transferring particle (or *Franck-Condon factors*, FCs), \hbar is the Planck constant (quantum of action) and H_{DA} are *transition matrix elements*, where the transition may be tunneling (but not necessarily!). In all cases disclosed here, transfer occurs between an initial (donor, D) and final (acceptor, A) state, and always within a protein environment that may be in a complex with a small molecule be it a substrate, odorant or chromophore. The transit can be treated classically, or with various degrees of quantum definition (e.g., of the electronic states and/or nuclear states). One tool, simple and effective for describing any transfer event is a *configuration coordinate* diagram as in figure 1, where a classical picture is illustrated.

In classical absolute reaction rate theory, Eyring 1935 [3], the rate constant of a transitioning particle from D to A , as in figure 1, would be given by:

$$k = \kappa B \exp \left\{ \frac{-\Delta G^\ddagger}{k_B T} \right\}, \quad (1.2)$$

$$k = \kappa B \exp \left\{ \frac{\Delta S^\ddagger}{k_B} \right\} \exp \left\{ \frac{-\Delta H^\ddagger}{k_B T} \right\}, \quad (1.3)$$

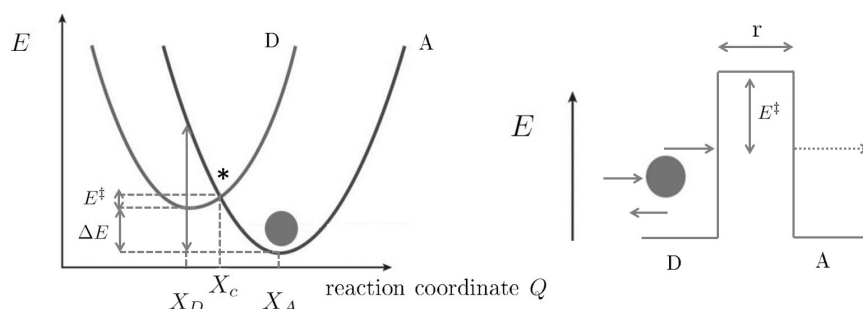


Figure 1. Left: a configuration coordinate diagram showing the activation energy barrier E^\ddagger , separating the reactant states (donor D) from the product states (acceptor A) which are shown as diabatic Born-Oppenheimer surfaces, with $\kappa = 1$, as in equation 1.2. Shown also; ΔE the energy difference at minimum between the D and A, at X_D and X_A respectively, λ the reorganization energy and the reaction coordinate Q [1], [2]. X_c indicates a crossing point for the transitioning particle at *. Right: a classical tunneling (or insulating) barrier that separates the donor and acceptor positions, barrier height is E^\ddagger , barrier width is distance r .

where $B \sim 10^{11} M^{-1} s^{-1}$ is the collision frequency of the reacting particles depending on the nature and phase of the mixture. The above relates to the Arrhenius equation [2]:

$$k = k_\infty \exp \left\{ \frac{-\Delta E^\ddagger}{k_B T} \right\}. \quad (1.4)$$

Where ΔE^\ddagger is the energy of activation, ΔG^\ddagger is the free energy, ΔH^\ddagger is the enthalpy and ΔS^\ddagger the entropy. Within this classical regime the factor $\kappa \mapsto |H_{DA}|^2$, see equation 1.1, and its value determines adiabaticity/non-adiabaticity, with $\kappa = 1$ or $\kappa < 1$ respectively, i.e., the nature of the Born-Oppenheimer surfaces (as depicted in figure 1. The configuration coordinate diagram shows these terms, and by the parabola geometry it can be found that $E^\ddagger = (\lambda + \Delta E)^2 / 4\lambda$ where λ is the *reorganization* (or relaxation) energy coupled to the particle transfer. The total reorganization energy is usually considered as a summation of inner shell atoms (i) and solvent molecules (o) re-arranging respectively, $\lambda = \lambda_i + \lambda_o$ where:

$$\lambda_i = \frac{1}{2} \sum_j k_{ij} Q_j^2, \quad (1.5)$$

and the Q s indicate harmonic oscillators, i.e., the displacement from equilibrium position upon charge transfer, as governed by Hooke's law where k_{ij} is a spring constant, assuming *normal mode* vibrations. The outer molecular environment re-arrangement is given by:

$$\lambda_o = \frac{(\Delta e)^2}{4\pi\epsilon_o} \left(\frac{1}{2r_1} + \frac{1}{2r_2} - \frac{1}{r_{12}} \right) \left(\frac{1}{D_{op}} - \frac{1}{D_S} \right), \quad (1.6)$$

where the charged particle, in this case, is an electron e and r is the radii of two reactants, r_{12} of the two reactants in contact, D_S is the static dielectric constant and D_{op} is the square of refractive index of reaction. The reorganization energy can be generalized to $\lambda = \mu\omega^2 Q^2 / 2$, where Q is a normal mode, μ is the reduced mass and $\omega = 2\pi\nu$ is the angular frequency of oscillation, examining figure 1, it can be seen that this reorganization energy is that energy required to displace Q without charge transfer, $Q = X_D - X_A$.

In the purely classical picture it is the case that for a transition $D \mapsto A$ there is a probability of occurrence determined mainly by overcoming the activation energy barrier E^\ddagger , and the ability of the environment to arrange such that there is crossing at X_c , and there is energy conservation $E_D = E_A$. That is if the particle is considered a ball as in figure 1. If the particle is considered a

wave; the probabilities change determined by the overlap of wavefunctions. The energy barrier depicted by the wall ΔE^\ddagger becomes penetrable: tunneling occurs. In the quantum mechanical penetration of a square barrier like in figure 1 [2], the probability of a particle penetrating is given by [4]:

$$P \propto e^{(-2/\hbar)\sqrt{2m\Delta E^\ddagger}r}, \quad (1.7)$$

such that the probability decays exponentially with increasing barrier width r and the decay constant varies with the square root of the barrier height ΔE^\ddagger and mass m of the particle. Thus in classical activation: the height of the barrier is the main hurdle, whereas in quantum activation: the width of the barrier is also an important obstacle, given the rate falls off exponentially with distance. This review highlights the use of this equation 1.1 for tunneling phenomena, as Oppenheimer first showed in 1928 [5], but applied to biology. Further it will be seen that various other effects in biological systems beyond tunneling, such as coherence (section 4) and entanglement (section 5) arise from the analysis of the rate equation and the determination of the Hamiltonian that defines the transition from D to A, H_{DA} .

(b) The environment, helps or hinders?

In the rate equation, the Hamiltonian H_{DA} may simply describe two eigenstates, D and A. In some cases this is enough to describe rate observations, in others a fuller definition of the Hamiltonian is required, which may be limited by what is definitively known of the system. In the field “quantum effects in biology” the Hamiltonian is that of an *open quantum system*: that is a quantum mechanical system that is influenced by its immediate environment:

$$H = H_S + H_E + H_I. \quad (1.8)$$

Here H_S is the Hamiltonian for the system, H_E describes the free evolution of the environment and H_I the interaction between the environment and the system [6]. If we are describing electron transfer for example, H_S may involve electronic states on D and A. In fact in equation 1.8 it most often is the case that H_S represents electronic states, H_E , the nuclear states and H_I the nuclear-electronic interactions. Such that the Hamiltonian is written so that electronic states are coupled to a ‘bath’ of nuclear motion that may be represented by a collection of (bosonic) oscillators as in equation 1.5 or as a collection of spin states see section 5. The Hamiltonian H (or H_{DA}) is considered “closed” if the system-environment evolves unitarily (see section (a)) but “open” if non-unitary (the environment, or protein’s, degrees of freedom are taken into account). The open quantum system thus accounts for the quantum effects of the protein dynamics on the rate (e.g. of charge/energy transfer), typically expected to dissipate and “leak” information.

Usually environmental variables are controlled where possible in physical tests, one variable is isolated and the effect of changes on the rest of the system monitored. Where quantum effects are typically observed, the system is usually a relatively simple, perhaps single molecule. In contrast biological systems, likely of many molecules (and atoms), degrees of freedom and so, *many* variables, are not simple. In the simplest forms the following examples constitute a particle (e.g. an electron, a photon) a ligand (or pigment) and a protein which hosts the interaction. Proteins have many degrees of freedom and so potential energy landscape, and are dynamical beasts which move within this multidimensional landscape. This environment is often in the literature referred to as a “wet, noisy and warm system” in contrast to the isolated, single molecule view that a solid state physicist may prefer. This wet warm noise, is thought to “drown” out any fine tuned quantum effect. Whatever an electron or a photon may be doing would be washed away by the large amplitude, governed by kT , of nuclear vibrations insensitive to the transitions in and around them. Fascinatingly, and contrary to expectations, it seems that, far from being insensitive to, or drowning out, these small effects, it is becoming clear that the protein environment is not only integral to, but *assists* these rate changes contrary to expectations. Such “protein-pigment-complexes” or PPCs will be described in the following four examples. Notably, only one such

PPC is depicted here, in figure 7, with protein data bank information (pdb code 3BSD). Structure data for PPCs are ubiquitous for enzymatic systems, but unknown in the case of olfaction and magnetodetection. Not unsurprisingly, much more testing of “quantum effects” has ensued in the (much larger, and growing, field) of photosynthesis. One reason being the photosynthetic materials present less challenges experimentally, but also they are more water soluble (more than olfactory receptors for example), available and cheap, e.g., spinach can be used to extract a light harvesting system for testing relatively easily.

2. Enzymes

Enzymatic processes are catalytic mechanisms in the body for essential biochemical processes e.g., hydrolysis of the neurotransmitter acetylcholine by the enzyme *acetylcholinesterase*. The paradigm for enzymatic reactions is the “lock and key” concept (see also section 3) derived from the fact that the enzyme substrate binds into an “active site” on the enzyme structure, making particular *intermolecular* contacts with amino acid residues on the enzyme. These residues typically act as nucleophiles or acid/base catalysts in the reaction, which occurs only if these point contacts are made: as a key (substrate) fitting into a lock (enzyme). Obtaining this particular arrangement, like a ‘lock and key’ or a ‘hand in glove’ between the enzyme and substrate, may involve orbital steering, and ‘pushes’ the substrate towards a Transition State (TS), along the reaction trajectory from the initial (reactant) to the final (product) state (or from D to A as in figure 1). This fit then drives a transition along a reaction pathway, on a configuration coordinate diagram and the activation energy of the reaction is lowered (see equation 1.4). The phrase for this process, first coined by Pauling [1], [7], is the “enhanced transition state theory”, so-called “enhanced” because of this preferential binding between enzyme and substrate, that cannot be easily mimicked or substituted. However, a confounding puzzle exists: the efficiency (or speed) with which this transition occurs (i.e., there can be 10^{25} fold difference in rate, experimentally observed, when comparing the molecules reacting in solution versus enzymatic environments [1]), cannot solely be explained by classical mechanics and any purely classical transition state theory (TST). Not only are these fast rates observed, but enzymatic processes exhibit weird behaviour with respect to temperature. How are these strange results and faster rates achieved?

Key experiments in 1966 by DeVault and Chance first showed that a *tunneling* effect was present in enzymes see figure 2 [8]. In *Chromatium Vinosum*, a photosynthetic bacterium, light-induced oxidation of cytochrome initiates electron transfer from cytochrome (donor, D) to bacteriochlorophyll, BChl (acceptor, A), see figure 2 for DeVault and Chance’s depiction of the path. Unless the two molecules are in close proximity (within Van der Waals contact), electron transfer from cytochrome to BChl is divided by a barrier, a classically forbidden/insulating barrier. The experiments showed that, as expected, the oxidation at high temperatures is temperature *dependent*; the rates are faster at higher temperatures indicating there is an activation barrier to surmount as in figure 1. But, surprisingly, at lower temperatures (100- 4K) the temperature dependence is lost, and the reaction still occurs without the “required” energy to overcome the TST activation barrier. This implies, that without the kick of kinetic energy to surmount the barrier, the electrons must be quantum mechanically tunneling through. This finding thus first highlighted the inability of TST in its classical regime to explain the temperature independence at low temperature *and* the high rates of electron transfer. Whilst increasing the temperature does increase the reaction rate, the classical theory still doesn’t account for the fastest rates. Quantum tunneling is one way to penetrate barrier crossing and so avoid the barrier height issue to enable and enhance a rate.

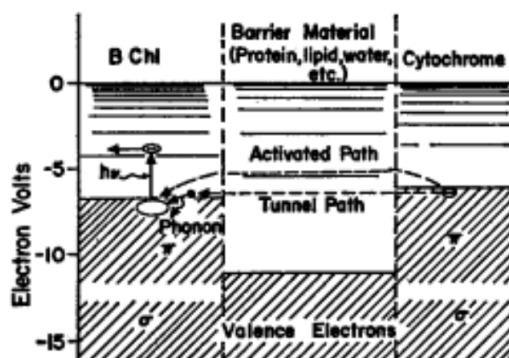


Figure 2. DeVault and Chance's pictorial description of the tunneling region between cytochrome and bacteriochlorophyll (BChl) from [8] with permission from Elsevier. Energetic levels occupied by valence electrons are shown. The BChl is excited by light $h\nu$ which leaves a hole quickly filled by an electron tunneling from the cytochrome. DeVault and Chance also indicate the possibility of an "activated" path versus the tunneling path, where the activated path may be enabled, for example, by a vibration in the cytochrome, bringing together the energetic states to the crossing point * see figure 1, and/or the tunneling path also may be "stabilized by a phonon emission" [8].

Are enzymes using quantum tunneling to enable and/or enhance their rates? One way to test the idea is with the Kinetic Isotope Effect (KIE); increasing the mass of an atom (where to within a suitable degree, all else remains the same) by isotopic substitution will alter the rate, in a mass (frequency dependent) manner given $v = \frac{1}{2\pi} \sqrt{\frac{k}{\mu}}$, where k is the force constant, μ the reduced mass and ω is the bond frequency, and $\omega = 2\pi v$. Heavier isotopes have lower frequencies v , a higher activation energy ΔE^\ddagger and so a lower rate- if determined by equation 1.4. Changing the mass in the rate equation determined by TST thus yields an expected rate change, e.g., for deuterium vs hydrogen (D/H) and tritium over hydrogen (T/H). So isotopic substitution allows a test for how well the observed rates can be predicted in a KIE:

$$KIE = \frac{k_l}{k_h} = \frac{A_l}{A_h} \exp \left\{ \frac{E^\ddagger(h) - E^\ddagger(l)}{RT} \right\}. \quad (2.1)$$

Where l denotes the light particle and h denotes the heavy particle, A is an Arrhenius prefactor, R is a gas constant and E^\ddagger is an activation energy (see figure 1)[1]. This rate equation attempts to explain the empirical evidence of the very fast rates and the seemingly odd temperature dependence, classically. However the rate constant deviations are not as expected. Indeed, deviations from the expected rate have been consistently observed in experiment, indicating quantum mechanical tunneling. Considering a hydrogen transfer event, see figure 3, [9]. It can be expected that as hydrogen would have a lower activation energy it will have a faster rate. Not considered in the classical regime is that it is more probable not just because of a reduction in the barrier height (activation enthalpy ΔE^\ddagger) but also a reduction in the distance of transition (width of barrier) r , see equation 1.7 and figure 1. Lighter particles can tunnel over larger distances. Heavier particles have comparably shorter de Broglie wavelengths: i.e., they are more susceptible to distance fluctuations and so do not tunnel as far. In 1989 Judith Klinman was the first to show proton tunneling in enzyme reactions using the Kinetic Isotope Effect (KIE) with consideration of full quantum mechanical vibrations to narrow the D-A gap (r) and facilitate tunneling, providing less width for more efficient tunneling which explains the increased rates better [10].

Using equation 1.1 and 1.4, and so treating the nuclear motion classically but the charge transition quantum mechanically:

$$k_{DA} = \frac{2\pi}{\hbar} \frac{1}{\sqrt{4\pi\lambda k_B T}} H_{DA}^2 \exp\left(-\frac{(\lambda - \Delta E)^2}{4\lambda k_B T}\right), \quad (2.2)$$

we acquire the non-adiabatic semi-classical Marcus theory expression which can be used in the high temperature limit (when all the vibrations are excited) $k_B T \gtrsim \hbar\omega_o$ [2], [11]. So transitions at high temperature can be measured and calculated for their rates, however, a fully quantum picture is required to determine the temperature independence at low temperatures as observed in the experiments by DeVault and Chance. At thermal equilibrium oscillations have large energy $k_B T$ with the square of standard deviation given by $\sigma^2 = \frac{k_B T}{k_i}$, and a probability of displacement from equilibrium given by:

$$P(x) = (2\pi\sigma^2)^{-1/2} \exp\left(-\frac{x^2}{2\sigma^2}\right), \quad (2.3)$$

accounting for quantum mechanical vibrations instead of classical, the average energy is given by:

$$\tilde{E} = (\hbar\omega/2) \coth(\hbar\omega/2k_B T), \quad (2.4)$$

such that, for the equally spaced vibrational quanta (phonons) of difference $\hbar\omega$, even at $n = 0$, the lowest energy level has $\hbar\omega/2$ and a probability of displacement:

$$\sigma^2 = (\hbar\omega/2k_i) \coth\left(\frac{\hbar\omega}{2k_B T}\right), \quad (2.5)$$

which converges to $k_B T$ at high temperature, $k_B T \gg \hbar\omega/2$ and $\hbar\omega/2$ at low temperature $k_B T \ll \hbar\omega/2$, where independence of T is achieved. So, now treating the nuclear vibrations as quantum, we arrive at the semi-classical regime [12]:

$$k_{DA} = \frac{2\pi}{\hbar} |H_{DA}|^2 (2\pi\sigma^2)^{-1/2} \exp\left(-\frac{(\lambda - \Delta E)^2}{2\sigma^2}\right). \quad (2.6)$$

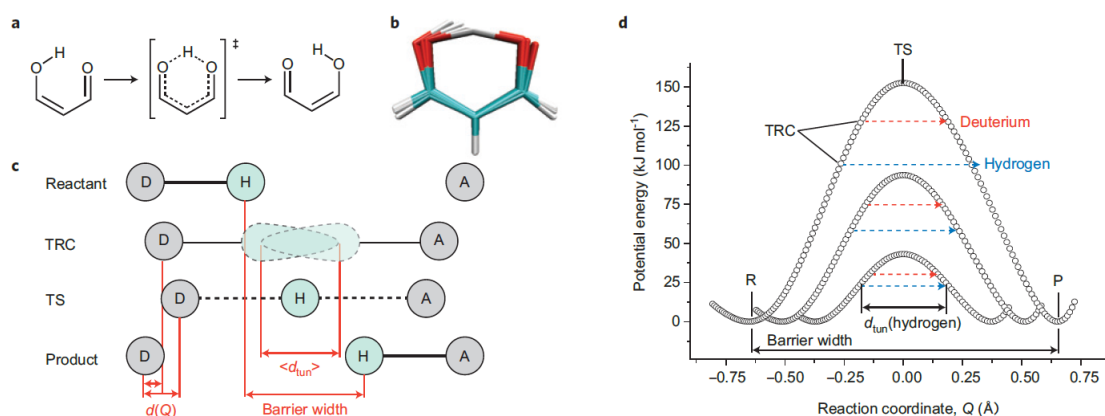


Figure 3. Showing the internal hydrogen transfer in malonaldehyde from Scrutton *et al* [9]. a and b show the transition towards product from reactant, via the transition state. c indicates donor (D) and acceptor (A) moving along a reaction coordinate, Q , the dashed line shows where tunneling is most probable at the transition state TS. The TRC denotes 'tunneling ready coordinate'. d shows the potential energy surface along a reaction coordinate for hydrogen and deuterium transfer at the same D-A distances. The idea of a "promoting mode": to enhance the hydrogen transition is depicted, if motion in c $d(Q)$ is conducive to promotion, then the tunneling distance d_{tun} is reduced and in combination with a lowering of the activation enthalpy a rate enhancement results.

The fully quantum regime can be obtained by using equation 1.1 with FC factors. Using FC factors that assume the Condon approximation, that the transition H_{DA} is constant over the cross-over region, see * in figure 1, and the nuclear and the electronic part of the Hamiltonian can be separated and factored out. As nuclear vibrations are on the scale of 0.1Å versus 1-10Å transit of a charge tunneling (for example) it is reasonable to suppose that charge feels a fixed field with respect to the nuclear environment. The full quantum transition rate was first determined by Huang and Rhys in [13], for F-centres in diamonds. It takes into account not just the probability of charge transfer due to the charge's ability to tunnel, but also with respect to the ability of oscillators to make quantum transitions that facilitate the processes. This is measured by the nuclear part, an *overlap integral*:

$$C(n, n') = \int \chi_n \chi_{n'} d\chi. \quad (2.7)$$

Where $C^2(n, n') = FC$, is a Franck-Condon factor, n' is a vibrational state on A and n is a vibrational state on D, χ is a vibrational wavefunction. Evidence provided by the C. Vinosum data, [8], is best fitted by the full quantum mechanical (QM) model:

$$k_{DA} = \frac{2\pi}{\hbar\omega} |H_{DA}|^2 \exp^{-S(2n+1)} \left\{ \frac{\tilde{n}+1}{\tilde{n}} \right\}^{\frac{1}{2}p} I_p \left(2S[\tilde{n}(\tilde{n}+1)]^{1/2} \right). \quad (2.8)$$

Where $S = \lambda/\hbar\omega = \mu Q^2 \omega / 2\hbar$ is a Huang-Rhys factor, \tilde{n} is the average quantum number of ensemble oscillators, I_p is a Bessel function, [14]. The full quantum consideration, equation 2.8, converges to the classical Arrhenius activation barrier, equation 1.4, in the limit of high temperature. Thus equation 2.8 explains the results at the higher temperatures but also the temperature independence at low temperatures. The experiments can most completely be explained by tunneling in enzymatic processes [1]. Further to experiments implying a quantum tunneling effect, modeling the process with a full quantum mechanical treatment fits the experimental results well [1, 15]. For example, for the process of ascorbate oxidation by ferricyanide, the observed KIE at room temperature is larger than the semi-classical limit by a magnitude ~7, indicating that nuclear quantum mechanical tunneling of the proton occurred (and it is perhaps vibrationally assisted)[16]. Thus calculating the rates of such charge transfer, with full quantum analysis not only converges to the classical result (the regimes are not mutually exclusive), but explains the empirical tests provided via isotopic substitutions.

(a) Challenges and future prospects

Though it is very well established that quantum mechanical tunneling plays an important role in enzymatic processes that sustain life, it is still the case that this information is not fully applied in the development of catalysts, for example, which scientists still fail to make as efficient as biocatalysis by enzymes. Partly this may be because it is not fully clear exactly what role the protein environment takes. As in photosynthesis see section 4 (and potentially olfaction, see section 3) it is becoming clear that the 'hot and messy' environment (the protein) may actually aid rates and transitions rather than hinder, in ways that have not been fully quantified yet. Protein conformations from equilibrium in a tunneling pathway may have very small destructive interference, they may also modulate the energy gap between donor and acceptor sites in the protein electron transfer reactions: thermal control can be helpful! An interesting notion of "promoting modes" versus "accepting modes" has been defined with respect to tunneling in enzymes [17], see figure 3 and 4. The latter meaning a non-vanishing overlap integral accounts for charge transfer, as in equation 2.7, i.e., the transition is *enabled*, versus the former which leads to active compression of the activation barrier, by reducing the height or the width, i.e., the transition may be *enhanced*. As in figure 3, a vibrational motion $d(Q)$ coupled to the reaction coordinate compresses the reaction barrier [17]. Identifying such promoting and/or demoting modes present in the protein's oscillating environment may be key to engineering better rates.

The development of terahertz spectroscopy that is able to determine single molecule vibrations may lead to a promising future in this area [18, 19].

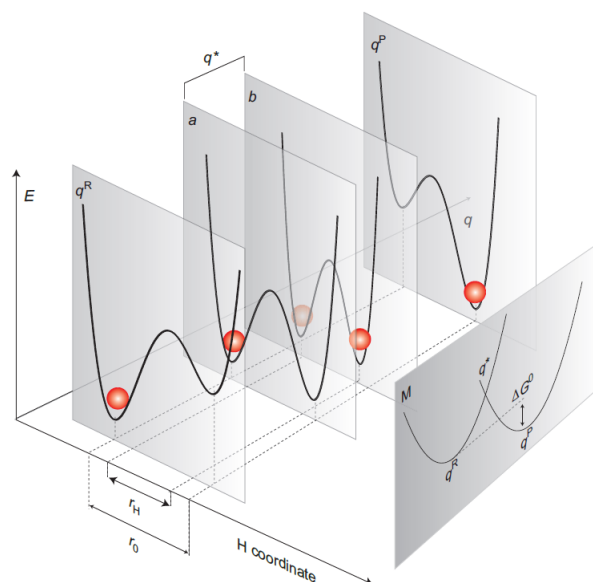


Figure 4. Depiction of vibrationally assisted models of hydrogen transfer from [9]. E denotes energy on the potential energy surface, q is the environmental reaction coordinate, r is the hydrogen coordinate where transfer is indicated by the red sphere, occurring at crossing point q^* . q^R denotes hydrogen in the initial/D state, and q^P the hydrogen on the final/A state. 'M' denotes this Marcus-like depiction, see equation 2.2, of the Born-Oppenheimer states on the environmental reaction coordinate. In a promoting mode a vibrational motion must be coupled to the itinerant charge.

3. Olfaction

In olfaction, the process by which we detect odor, it is not fully understood how an odorant molecule *initiates* the odorant response. It does so by “turning on” an olfactory protein, a G-protein coupled receptor (GPCR) [20], but the physical mechanism by which it does this has not as yet been fully determined. One theory is that the odorant fits the receptor like a “lock and key”, similarly to the previous section 2, however, designing odorants based on such shape complementarity between receptor and odorant (analogous to the substrate and enzyme) proves that this theory alone is not sufficient in the case of explaining olfactory response [21]. For one thing very diversely shaped molecules can initiate the same receptor and conversely same-shaped molecules initiate non-mutual receptors, such that the receptors are often referred to as simultaneously “discriminatory” and “promiscuous”. Further, olfaction does not alter the chemical composition of the odorant, there is no driving toward a product state from a transition state (in the odorant at least) like in TST. There are ~ 390 types of functional human olfactory receptors, [22], all of which are somehow “tuned” to respond to the different molecular stimuli offered by odorants in order to span a “smell space” of potentially thousands of odorants [23], and they do so in a combinatorial process: many receptors initiated constitute a “code” that determines a smell character [20]. The receptors do this consistently (there is no subjectivity at the receptor level), and are shown to be exquisitely sensitive to “something” of the odorant (in ~ 390 ways), but that something is currently unknown. This is not a unique problem to smell: many ligand-protein recognition events are not well understood, and notoriously rational design of drugs based on “structure activity” relationships fail to come up with successful lead candidates.

Since GPCRs are an important drug targeting class, ~50% of pharmaceutical designed are targeted at this class of protein [24], advancement in this area is of great importance to global health. Determining a completed theoretical basis for molecular recognition, when the ligand is not chemically altered, that is truly explanatory and predictive is an ongoing process.

It was first proposed by Dyson and then Wright [25, 26], that this “something” could be the odorants molecular vibrations: that the receptor is somehow transducing the thermal fluctuations of an odorant. However, as everything in biological processes is thermally fluctuating, how would the receptor extract this information from the noise? Later, Turin [27], proposed that the receptor is detecting the odorants *quantum mechanical* vibrations. This process had already been established as a signaling transduction mechanism by Jaklevik and Lambe, [28] in 1968, where they showed inelastic electron tunneling (IET) through a small molecule, that bridges an electrode junction, encodes information of the molecular energetics (quantized vibrations, or phonons) in the resulting current, see figure 5.

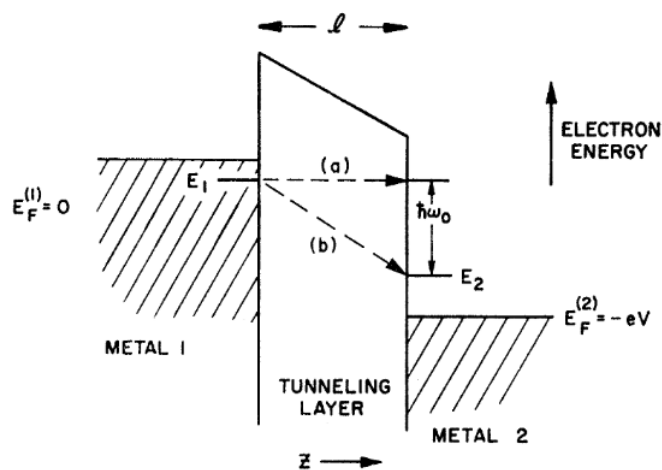


Figure 5. Lambe and Jacklevic demonstrate inelastic electron tunneling through a metal junction, from [28]. There are two possible ways for the electron to cross the tunneling layer (insulating barrier) via a) an elastic or b) an inelastic transition. The inelastic transition occurs when there is a molecule bridging the tunneling layer with a mode of vibration, $\hbar\omega_0$, that the tunneling electrons excites, and so loses energy to.

In IET there are two possible ways for the electron to cross the tunneling layer via a) an elastic or b) an inelastic transition. In the elastic case the electrons tunneling across the insulating barrier (in the figure 5 see “tunneling layer”) do so without losing energy, transitioning from one Fermi level to the other in crossing from metal 1 to metal 2. In the inelastic case the electron loses energy that directly matches whatever may be filling the insulating barrier, such as a molecular “bridge” with an excitable mode of vibration. Typically the elastic current is dominant and can be extracted from $\frac{I}{V}$ plots, whereas the inelastic channel is extracted from the second derivative, $\frac{d^2 I}{dV^2}$, as peaks in the spectra that correspond to increases in conductance due to vibrational modes $\hbar\omega_0$, thus identifying what molecule fills the tunneling layer by its spectrum. Turin’s proposal was that the GPCR olfactory receptors implement a similar mechanism [27]. Since, it has been established that a mechanism for biological IET is feasible as a detection mechanism in the nose if you consider Fermi’s golden rule for electron transfer where the odorant is treated as a small perturbing presence [29]. Fermi’s “golden rule”, see equation 1.1- we refer to again, is a non-adiabatic rate equation that allows calculation of the times of a transition event (such as an inelastically or an elastically tunneling electron). The rule holds provided there is only weak

electronic coupling between two electronic states φ_D and φ_A , e.g. an electron in an initial state on a donor and in the final state on an acceptor (both fixed) and there is a separation of D and A energy levels, e.g., as in a binding site of a GPCR (or in the contacts between enzyme-substrate). Similarly to the metal junction in figure 5, the hypothesis is that an odorant docks at the GPCR binding site and fills an insulating barrier. A donor and acceptor state for electrons must exist somewhere in the odorant-receptor system such as a residue that hydrogen bonds to the odorant at the binding site (where the protein replaces the metal junction in this instance). The binding event and presence of the weakly coupled states at reasonable electron tunneling distances [4], enable the transfer of an electron due to the perturbing effect of the odorant's presence. The key question, however, is whether the electron transfer is elastic (not discriminatory - no energy loss) or inelastic (discriminatory - $\hbar\omega_o$ is lost) and so if the odorant molecule can be identified by its phonon excitation, or whether the non-identifying elastic route dominates, as in the metal junction IETS, disguising the odorant's effect.

Using Fermi's golden rule in this way results in a non-adiabatic semi-classical Marcus theory expression for olfaction:

$$k_{DA} = \frac{2\pi}{\hbar} t^2 \frac{\sigma_n}{\sqrt{4\pi\lambda k_B T}} \exp\left(-\frac{(\epsilon_n - \lambda)^2}{4\lambda k_B T}\right), \quad (3.1)$$

c.f., equation 2.2, except the particular parameters for olfaction, where $\epsilon_n = \epsilon_D - \epsilon_A - n\hbar\omega_o$, ϵ_D is the energy state of the donor, ϵ_A the acceptor, and $\hbar\omega_o$ is the vibrational mode of the odorant, $n = 1$ corresponds to one phonon excitation, $n = 0$ corresponds to zero phonon excitation on the odorant. $\sigma_n = \exp(-S)S^n/n!$, is a Poisson's expression for the dependence on Huang-Rhys factors S , $\lambda = \sum_q S_q \hbar\omega_q$ is the relaxation (or reorganization) energy of the environment, S_q is the Huang-Rhys factor for all the oscillations in the environment and S is the Huang-Rhys factor similar as in equation 2.8, but explicitly for the odorant. In the olfactory theory it is the ratio of the change in energy to $\hbar\omega_o$, where the change in energy is due to the change in force occurred to initiate the electron transfer due to the odorants perturbing presence, i.e., the 'kick' to cause the transition. Notice that again the Born-Oppenheimer principle is used: the electronic and nuclear wavefunctions are separated as usual in Marcus theory [30]. There is an electronic coupling matrix element contained in t that determines the strength between D and A at the nuclear configuration of the transition state and is sensitive exponentially to distance [4]. In the case of olfaction, a hopping integral between D and A is estimated, resulting from an admixture of these states with the odorant. The rest of the terms are Franck-Condon factors that determine the nuclear rearrangement upon electron transfer, and can be portrayed in a configuration coordinate similarly to figure 1, [31]. The crucial result is that the inelastic tunneling rate is higher (preferable) than the elastic rate. In other words when an odorant with a phonon of $\hbar\omega_o$ docks at the receptor with a donor-acceptor energy gap matching this energy then vibrationally assisted tunneling occurs- the electron is aided in its transition by the presence of the odorant. With no odorant present (or one with an 'incorrect' $\hbar\omega_o$), the tunneling event is less likely, thus quantum mechanics enhances the rate in order for discrimination: smell! This result has been replicated [32], and extended further by Nazir *et al* [33], from the original hypothesis beyond the semi-classical Marcus theory of [29] to solve a polaron master equation and find that accounting for dissipation by introducing a Lindblad term, see section 4, *increases* the frequency resolution of the receptor and the sensitivity to the presence of the odorant. It can be seen that, against intuition, dissipation assists the population of acceptor over donor states and the quantum dynamics of the system are more thoroughly accounted for in this model. The dissipative model also explains the phenomena of chiral recognition in olfaction [34], [35].

Any vibrational based theory of olfaction offers a simple test (similar again to the above section 2), provided by isotopic substitutions. Substituting atoms in the odorant enable a change in mass (and so frequency) that will shift the mode of vibration (e.g by 700 cm^{-1} [36], 86 meV), whilst keeping other physical properties the same, binding to the receptor for example, should not be significantly disturbed. Changing the vibration should alter the smell (which would be hard to explain classically). However evidence in this area is ambiguous. Haffenden *et al* [36] in

1996 showed that human subjects could distinguish benzaldehyde from benzaldehyde-d₆. Then in 2004 Keller and Vosshall reported that human subjects could *not* distinguish acetophenone and d-8 acetophenone [37] and then more recently in 2013 [38] this was contested and it was shown that in fact these particular isotopes *could* be differentiated when expert smellers and gas chromatography (for purity) were used. Note also behavioural studies using insects have suggested that *drosophila melanogaster* (fruit flies [39]) and *apis mellifera* (honey bees [40]) are able to distinguish isotopically substituted odorants. Such behavioural studies of insects evade the subjectivity elements unavoidable in human tests, but still do not isolate the effects at the receptor level, where there is no room for contention. One recent study by Zhuang *et al* [41], does just this, one of the ~390 receptor types they screened (“OR5AN1” identified as a human “musk-recognizing” receptor) is tested *in vitro* against deuterated and non-deuterated muscone. This test eliminates any process in perireception and post reception and directly probes the odorant-receptor activation process. They show for a number of musk odorants that dose-response curves do not show any differentiation between isotopic forms of the odorants with any statistical significance, see for example figure 6 [41]

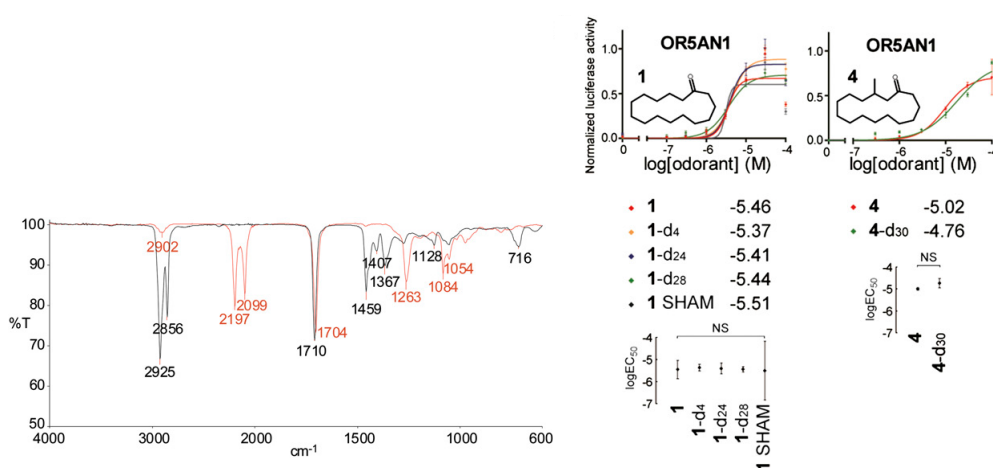


Figure 6. IR spectra for “4-d₃₀” (red line) and undeuterated muscone “4” (black line) indicating differing vibrational modes (particularly in the 1,380-1550 cm⁻¹ region) from [41] copyright Proceedings of National Academy of Sciences, USA. Also shown are dose-response curves of OR5AN1 plots for (1) cyclopentadecanone and (4) muscone and the scatter plots with 96% confidence interval log EC₅₀ values, showing there is no differentiation between isotopes that is statistically significant [41].

This study shows definitively that the muscone receptor is not sensitive to deuterated muscone odorants. This work is fairly damning for any vibrations based theory of olfaction, note however it concentrates on one particular “musk-sensitive receptor” and further it tests the hypothesis that C-H vibrations alone are signatures in smell spectra. According to the theory developed [29], it would a better test to probe vibrational modes such as C=O, for example (substitute with isotopic oxygen), which are more likely responsible for the large changes in forces (there are larger moving partial charges upon phonon excitation) that would give rise to an enhanced electron tunneling event (or *promoted*, as in section 2). It is likely in all these (C-H targeted) deuteration experiments, the wrong mode of vibration is being tested- one that would not typically stand out against others in the odorant-receptor environment. This concept is explored in Lin & Besohn 1968, as in section 2, showing that ‘promoting modes’ in naphthalene and acetophenone correspond to C-C stretching vibrations which give appreciable derivatives of electronic wavefunctions with respect to the nuclear coordinates, as opposed to the C-H stretching vibrations which provide ‘accepting modes’ (non-vanishing overlap integrals), [42]. Both can occur but, the promoting state

is better at enhancing the rate, or perhaps in the case of olfaction being the signature vibration that turns “on” the receptor.

(a) Challenges and future prospects

Apart from the recent study by Zhuang *et al* which concentrates on muscone [41], there has been little experimental testing of the vibrational theory in smell. Testing various isotopic substitutions in this manner at the receptor level would be very informative. Any detailed quantum mechanical analysis of the binding site in olfaction is limited by the lack of crystal structures available for the olfactory receptors. Energy states ε_D and ε_A are assumed to be molecular orbital states (highest occupied molecular orbitals). Is it even possible for an energetic donor-acceptor splitting to match such a small $\hbar\omega_o$ (typically 200 meV)? What donors and acceptors of electrons might there be available in the olfactory receptor? Calculating the electronic coupling for initial and final wavefunctions without any structural information would constitute very involved guesswork, given structural fluctuations on the picosecond timescale and sub-Ångstrom distances may substantially affect any quantum process. However, recent studies have advanced knowledge of the binding site [43] and new research is emerging to show that biological IETS may play a role in neuroreceptors [44]. So let the notion of phonon assisted electron tunneling (as a signalling mechanism) be emphasized and not ignored, if not a role in olfaction, but perhaps in other systems in biology that rely upon ligand-receptor activation.

4. Photosynthesis

Photosynthesis, abundant in plants, algae and bacteria, is arguably one of the most important fundamental interactions on Earth: the conversion of sunlight energy into the chemical energy that forms the basis of life. In brief, a photosynthetic system uses an “antenna” (100,000s of light absorbing molecules) to capture sunlight energy which initiates the process by creating an “exciton”; an electron-hole pair, that travels to the Reaction Centre (RC) and ultimately results in the production of ATP, the “molecule of life”. For maximum efficiency all photons absorbed have to make it to the RC; but there are so many random paths! The photon does not “know” the most efficient route. So the suggestion is that, rather than taking one path, quantum coherence is used to travel all paths simultaneously. Given the photosynthetic molecule’s *raison de être*, often if surviving in hostile (low-light level) conditions, is to gather as many photons of light at the RC as possible- what benefits are provided by quantum physics? One possibility is that coherence and interference exhibited by the absorbed photons may enable a quantum “random walk”- most efficiently getting the energy to where it needs to be [45]. This process is *electronic energy transfer* (EET), rather than energy transfer, but equation 1.1 can again be used to calculate transfer rates.

These first photosynthetic steps: energy harnessing and transfer to the reaction centre for charge separation, all take place within 10’s of ps. The protein-pigment complexes (PPCs) that constitute the antennae that funnel the excitation energy to where it needs to be are exquisitely manufactured such that these systems may operate at low light levels and still gather enough excited states but conversely they must be able to operate in excess sunlight, and therefore contain “quenching” molecules that protect against light damage. The key chromophoric pigments in photosynthesis (those that absorb photons to make an “exciton”) are chlorophylls, for example as in figure 2, the primary molecules in photosynthesis. However, carotenoids are often in close proximity in order to “tune” energetic states, like the protein may do in olfaction and/or enzymatic processes. Carotenoids actually most often serve as regulatory molecules, they photoprotect chlorophylls from population of triplet states in excess light conditions so that damaging free radicals are not generated.

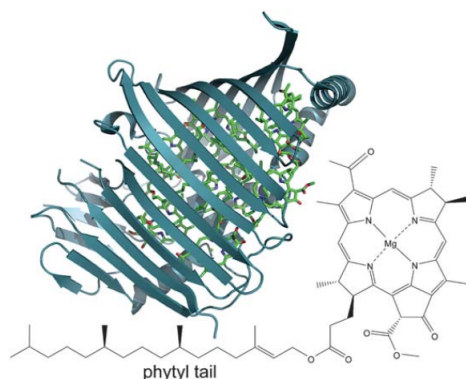


Figure 7. A PPC from pdb code 3BSD showing the 7 pigments in the Fenna-Matthews-Olson (FMO) complex in *Chlorobaculum tepidum* (formerly *Chlorobium tepidum*) from [46]. The structure of the FMO is shown in blue ribbon and the chromophores: bacteriochlorophyll a (BChl a) is in green. The 2D molecular structure of the seven BChl a is also shown next to the protein [46].

Figure 7 illustrates the structure of the Fenna-Matthews-Olson (protein) complex and seven bacteriochlorophyll a (pigment) molecules from *Chlorobaculum tepidum*, a photosynthetic green sulphur bacteria. The FMO shown here is a monomer unit that exists in trimeric form in nature and links the chlorosome to the RC. The BChl a pigments absorb light at 800 nm which is referred to as the Q_y transition. Passing this excitation energy on to other pigments *en route* to the reaction centre, without fluorescing or being lost to any other route is integral to the efficiency of the overall process.

In the case of such a PPC the Hamiltonian for FMO, see section (b), H_{PPC} (or H_{DA}), is given by [47]:

$$H_{PPC} = \sum_{m=1}^N \sum_{a=g,e} H_{ma}(x) |\varphi_{ma}\rangle \langle \varphi_{ma}| + \sum_{m,n} \hbar J_{mn} |\varphi_{me}\rangle \langle \varphi_{mg}| \otimes |\varphi_{ng}\rangle \langle \varphi_{ne}|, \quad (4.1)$$

where there are m^{th} and n^{th} pigments (7 in total in the FMO case, though 8 have more recently been discovered) and they are either in the ground g or first spectroscopically excited state e . It is assumed there is no orbital overlap between these pigments and that the assignment of electrons is unambiguous. Wavefunctions $|\varphi_{me}\rangle$ and $|\varphi_{mg}\rangle$ (or donor D and acceptor A surfaces, as similarly to previous sections) are the initial and final (ground and excited) states as depicted in figure 9 and 8. $\hbar J_{mn}$ determines the electronic coupling between pigments and:

$$H_{ma}(x) = \varepsilon_{ma}(x) + \text{nuclear } k.e \quad (4.2)$$

is the Hamiltonian for nuclear dynamics as determined by the electronic state g/e and $\varepsilon_{ma}(x)$ is the potential energy as a function of the nuclear coordinates. $H_{mg}(x)$ and $H_{ma}(x)$ are modeled as set of displaced harmonic oscillators as in equation 1.5 and figure 1 and figure 8, represented by parabolas.

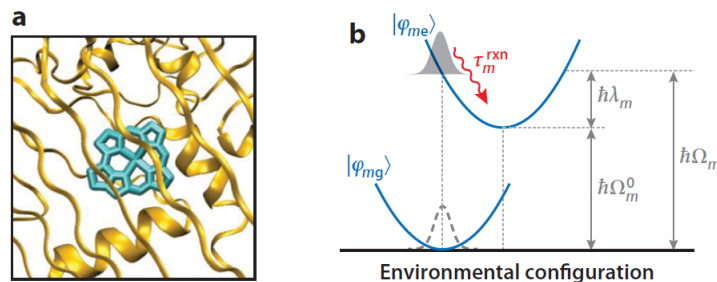


Figure 8. One BChl a pigment depicted in the FMO, and configuration coordinate diagram for the excitation process from [47], as an energetic excitation causes a transition from D or $|\varphi_{mg}\rangle$ to A or $|\varphi_{me}\rangle$. After excitation reorganization takes place with an energy $\hbar\lambda_m$ and timescale τ_m^{rxn} .

See in figure 8 that $\hbar\Omega_m = \varepsilon_{me}(x_{mg}^0) - \varepsilon_{mg}(x_{mg}^0)$, which is a Franck-Condon transition energy (or ‘site energy’ on the BChl a) and $\hbar\lambda_m = \varepsilon_{me}(x_{mg}^0) - \varepsilon_{me}(x_{me}^0)$ with reorganization time τ_m^{rxn} . Equation 4.1 contains many degrees of freedom so often environmental motion is modeled as random fluctuations. This is termed the “energy gap coordinate”, $u_m = H_{me}(x) - H_{mg}(x) - \hbar\Omega_m$ and determined by $u_m(t) = e^{iH_{mg}t/\hbar} u_{me} e^{-iH_{mg}t/\hbar}$. The choice of $u_m(t)$ is determined by fluctuations of normal modes at temperature T , moderated by dissipation characterized by a response function $\chi_m(t)$ that approaches the classical limit:

$$\chi_m(t) = -\frac{d}{dt} \Gamma_m(t), \quad (4.3)$$

and:

$$\chi_m(t) = \frac{i}{\hbar} \langle [u_m(t), u_m(0)] \rangle_{mg}, \quad (4.4)$$

where $\Gamma_m(0) = 2\hbar\lambda_m$, is the Stokes shift at high T [47]. This is termed the classical fluctuation dissipation relation (equation 4.3). The root mean square amplitude of the electronic energy gap is moderated by $\sqrt{\langle u_m^2 \rangle_{mg}} = \sqrt{2\hbar\lambda_m/\beta}$, at very large amplitude oscillations the quantum superposition state is collapsed and the classical solution is obtained. When $\hbar J_{mn} < \hbar\lambda_m$ or $\tau_m^{rxn} \ll J_{mn}^{-1}$ then the inter-pigment coupling is small with respect to the relaxation in the environment. In this small coupling limit the electron-nuclear coupling can be treated perturbatively: nuclear reorganization occurs before energy transfer (EET) and the motion can be described as incoherent hopping - a diffusive random walk. Within this regime we obtain a reaction rate, [48]:

$$k_{m \rightarrow n} = J_{mn}^2 \int_{-\infty}^{\infty} \frac{d\omega}{2\pi} A_m[\omega] F_n[\omega], \quad (4.5)$$

which shares similar characteristics to the rates derived in the sections 2 and 3. Equation 4.5 describes second order perturbation theory or Förster theory. FC factors are used to separate out the vibrational overlap and spectral features indicating that vibrations modulate EET, again similarly as to section 2. This scenario is otherwise known as “environment assisted” or “dephasing assisted quantum” transport. $A_m[\omega]$ is the fluorescence spectra of the acceptor pigment $F_n[\omega]$ is the fluorescence spectra of the donor pigment and the integral consists the “overlap integral” or “spectral overlap” as in equation 2.7, and the rate of transfer from pigment m to n is proportional to J_{mn}^2 .

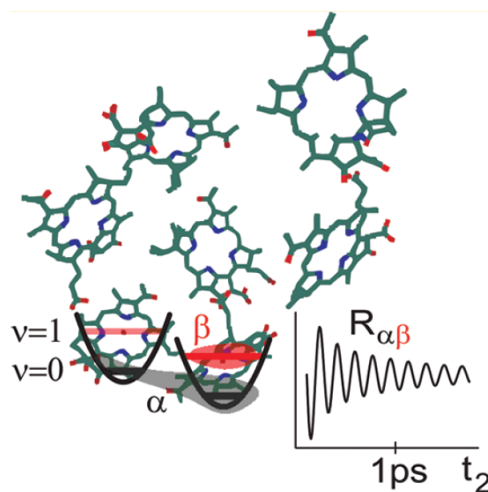


Figure 9. 7 BChl a's in FMO, with excitation states depicted and "quantum beat" oscillations with time, from [49].

It is not necessarily the case that the pigment coupling is small. In the case $\hbar J_{mn} > \hbar \lambda_m$, or $J_{mn}^{-1} \ll \tau_m^{txn}$, the non-Förster (Redfield) regime, the pigment excitation may be delocalized over several pigment sites and so the exciton is robust with respect to dissipation of the reorganization energy. In this case coherent transfer is observed where the exciton wave packet travels with phase coherence. To understand this coherent effect: referring to the full interaction system Hamiltonian, equation 1.8, where H_S is the Hamiltonian for the degrees of freedom in the system, H_E describes the free evolution of the environment and H_I the interaction between the environment and the system [6]. In the case of FMO:

$$H_S = \sum_m \hbar \Omega_m B_m^\dagger B_m + \sum_{m,n} \hbar J_{m,n} B_m^\dagger B_n, \quad (4.6)$$

is the Hamiltonian for the excited state of the pigments. The environment Hamiltonian is usually described, again, as a collection of harmonic oscillators that can be described by the bosonic relation, when the nuclear motion is quantum [48]:

$$H_E = \sum_m H_{mg}(x), \quad (4.7)$$

and the excitation-environment interaction Hamiltonian is given by:

$$H_I = \sum_m u_m B^\dagger B_m, \quad (4.8)$$

using the creation and annihilation operators $[B_m, B_n^\dagger] = \delta(m - n)$.

A third alternative to the Förster hopping regime or the above very strong coupling (or Redfield) regime is the intermediate regime where $J_{mn}^{-1} \sim \tau_m^{txn}$, which also exhibits coherent effects where the pigment excitation energy straddles all sites, see figure 10 for a representation of these three main regimes for EET, [50]. There are many models and techniques used to solve the Quantum Master Equation (QME, when the open system is evolved) for the understanding of wave coherence in photosynthetic apparatus, more thoroughly explained in these reviews [48, 50]. Förster and Redfield theory are second order perturbative methods used for small and very large electronic couplings, J_{mn} , respectively, and are only touched on here. The QME may also be solved for the intermediate regime, see figure 10, using the multiconfiguration time-dependent Hartree algorithm [50], and other techniques are the *generalized* quantum master equation, the path-integral approach, mixed quantum classical approaches and semi-classical methods [50].

Also hierarchical equations of motion (HEOM) and interpolates between the Bloch-Redfield and Förster regimes [50]. This surge in theoretical development is vast and complex so this review will serve only to point the interested reader to more thorough sources of study, whilst briefly outlining in the next section the reason for this great flurry of theory development: the experimental observation of coherent EET via 2D spectroscopy.

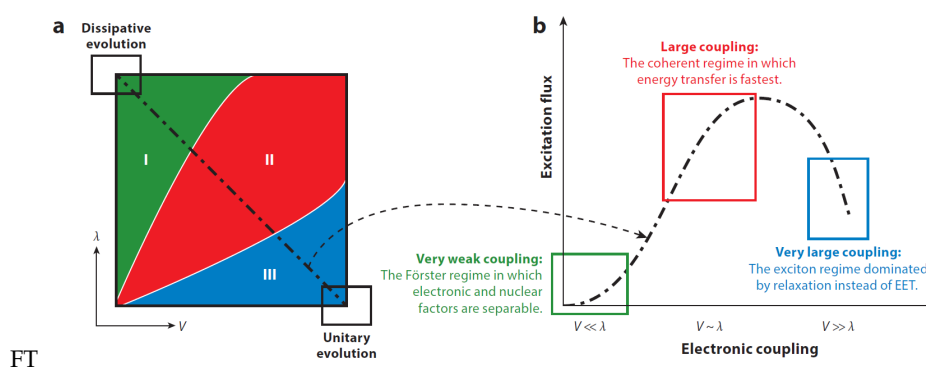


Figure 10. Figure to show the incoherent Förster (very weak coupling), intermediate coherent (large coupling) and Redfield (very large coupling) regime for EET in photosynthesis, from [50].

(a) 2D electronic spectroscopy

The FMO example, as in the above section, is so important because it was the first photosynthetic system to display long-lived coherent excited states in experiment [51]. Ultrafast (femtosecond) laser pulses are able to populate excitonic states within the BChl a Q_y band. Using $\Delta E \Delta t \sim \hbar$, the energy gaps of 70-400 cm^{-1} correspond to time periods of 80-500 fs [47]. A third order coherence response is generated by 3 pump pulses from a laser. Results are frequency and phase resolved using frequency domain heterodyne detection, obtaining a magnitude and phase of the signal. When the 3 laser pulses are directed at the sample, the time period between the first two pulses allows a 'one-quantum coherence' τ (the coherence time) between the ground and resonant excited states. The second pulse promotes population of more excited states, ground states and coherences between 'zero-quantum coherences'. The time period between the second and third pulse is the 'waiting time' T . The third pulse causes a radiative coherence (the third order coherence response). The period between the final pulse and the emitted signal is the rephasing time t . 2D spectra is taken at specific waiting times T , see figure 11. The 2D spectra is generated by fixing T and taking a 2D Fourier transform over the t and τ times [47].

The important point to note from these experiments, shown clearly in figure 11 for a marine cryptophyte algae (PC645) and in figure 12, where it was discovered for the first time in FMO, [51], is the fact that the amplitude of the signal is oscillating with time - quantum coherent "beats" are observed.

To understand the nature of these quantum beats we return to the system Hamiltonian, equation 1.8, which can be evolved with time as in $u(t) = \exp[-iHt]$, making a unitary transform operator $\rho(t) = u(t)\rho'(0)u^\dagger(t)$ for a density matrix in any basis set [47]. The equation of motion for the density matrix is the Liouville-von-Neumann equation for time evolution of an isolated (closed) quantum system:

$$\frac{\partial \rho(t)}{\partial t} = \frac{-i}{\hbar} [H(t), \rho(t)], \quad (4.9)$$

giving a first order differential equation, with operator L , the QME [6]:

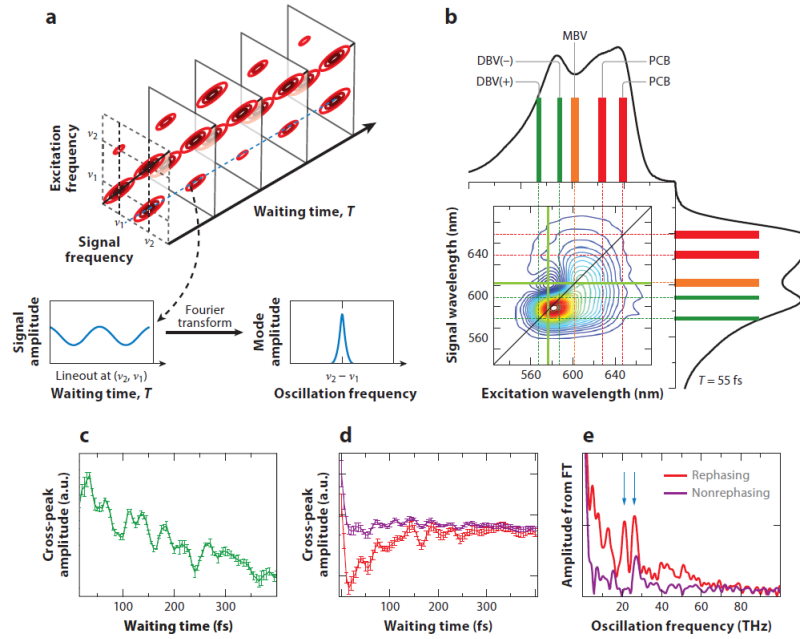


Figure 11. 2D electronic spectroscopy, in a) showing the time evolution of excitation between 2 pigments, “cross peaks” amplitudes oscillate with $\nu_2 - \nu_1$, Fourier transform gives the oscillation frequency. b) shows the 2D spectra at $T=55$ fs (real part of total signal) for PC645, a marine cryptophyte algae that contains 8 bilin (chromophore) pigments, coloured bars are peak absorptions for the chromophores. The green cross indicates a cross peak with coherent oscillation as a function of waiting time T (at 570 nm, 600 nm). c) plots the oscillation’s amplitude with waiting time d) plots the rephasing (red) and non-rephasing (purple) amplitudes of this cross peak and e) is a Fourier transform of the traces in d) showing that peaks occur at 26 THz in both signals but 21 THz only in the rephasing spectrum, from [50].

$$= \frac{-i}{\hbar} L\rho(t), \quad (4.10)$$

when expressed in the Hamiltonian eigenbasis with ε_i as the energy of the i^{th} eigenstate:

$$\frac{\partial \rho_{ij}}{\partial t} = \frac{-i}{\hbar} (\varepsilon_i - \varepsilon_j) \rho_{ij}, \quad (4.11)$$

$$\rho_{ij}(t) = e^{\frac{-i(\varepsilon_i - \varepsilon_j)t}{\hbar}} \rho_{ij}(0), \quad (4.12)$$

It can be seen that under time evolution of the reduced density matrix $\rho_{ij}(t)$ [47], that there are oscillations or “beats”, that are coherent for the off-diagonal elements of the density matrix that represents the ensemble $i \neq j$ (the transfer terms), and diagonal elements are the populations of energetic (spectroscopic) states $i = j$ which remain constant (energies of individual sites). For an observable to be measured (in spectroscopy) $\langle A \rangle = \text{Tr} \langle \hat{A} \rho \rangle$ the observable operator is the dipole moment change and is determined as the amplitude intensity, see vertical axes in figures 11, 12 and 13. The dipole moment operator does not commute with the Hamiltonian and so off-diagonal elements (the coherent beats) will be observed in measurements of the amplitude with respect to time, as is seen in the experiments. As noted, ways in which to solve the QME using various approximations to understand observed coherences are diverse and extensive. QMEs implementing a Lindblad operator, a *non-unitary* evolution of the density operator, which introduces a dephasing rate and the mixing of states, have been successfully studied in various

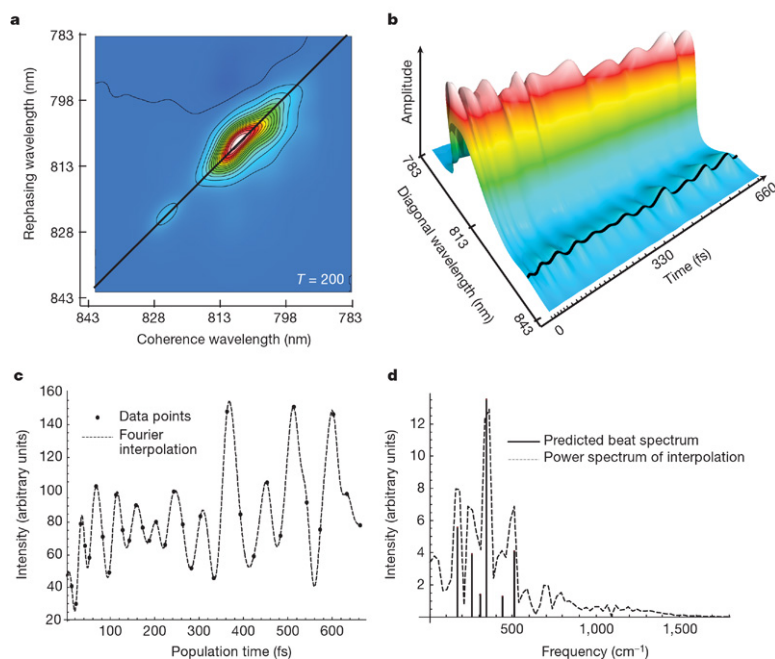


Figure 12. The first evidence of electronic coherence between single states in FMO, a non-rephasing signal appears on the main diagonal in a) and evolved in time, see b). Plotting the amplitude of the lowest exciton peak beating with time, upon Fourier transform d) reproduces frequencies that agree well with the predicted beat times and intensities, from [51].

elegant theoretical investigations that match well the 2D electronic spectroscopy observables [52, 53, 54, 55], but similarly Bloch-Redfield equations explain and predict observations well [56].

(b) Challenges and future prospects

The development of femtosecond (“ultra-fast”) spectroscopy, see section (a), in probing photosynthetic complexes has been a major break-through in the field “quantum effects in biology”. It shows the first instance of observing quantum superposition and coherence dynamics in vital biological systems. Though the discoveries have not been without dispute. There are debates on the mis-match between laser excited states generated in experiment and the natural continuum that comes from sunlight- are the coherent states even initiated in nature? Sunlight has a maximum intensity at 500 nm on the surface of the Earth [47]. Further, it has been discussed that 2D spectroscopy does not differentiate electronic coherence from vibrational. However this has been tested, where Hayes *et al* show isotopic substitution (again changing vibrational states) fails to affect the quantum beating [46]. It is thus surmised that the effect is purely electronic. The final main objection is: what about physiological temperatures? This has also recently been addressed, the first to show quantum coherence at higher temperatures ($> 77\text{K}$) was in phycobiliproteins in cryptophyte algae [46], and further in FMO itself, [57] even at room temperature quantum beats are observed, see figure 13.

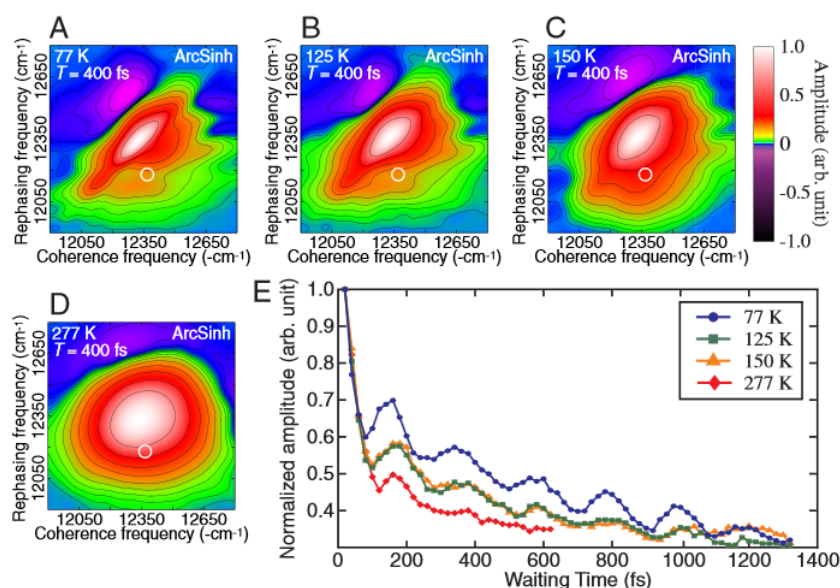


Figure 13. Quantum beats at room temperature in FMO from [57], copyright Proceedings of National Academy of Sciences, USA. Data shown are at waiting time $T = 400$ fs and A) is 77 K B) 125 K C) 150 K and D) 277 K. At higher temperature peaks are broader (dephasing between g and e states). Theoretical analysis, [58], extracts the quantum beat at the cross peak (white circle) and plotted in E) as a function of waiting time T to observe the amplitude oscillating. The beat occurs ~ 200 fs even at room temperature.

Though the temperature question seems to survive testing, coherent beats persist in ambiance. It is still questionable quite what is the point of long-lived electronic coherent states? If they are generated by natural light in photosynthetic systems, then why? It was initially thought that the coherence enables a faster search for the most efficient route to the RC, analogous to a ‘‘Grover’s’’ search algorithm, as borrowed from quantum information theory [45]. Essentially it appears plants are able to use algorithms to determine fast routes of the energy to the RC: in similar ways in which researchers would like quantum computers to work. Thus it has been predicted that there is much potential in quantum computing that biological mimetics may enable progress in generating photocells for clean energy transport.

5. Bird magnetoreception

Ornithologists Wolfgang and Roswitha Wiltschko were the first to observe and carefully document evidence, in the 1970s, of the phenomenon of bird migration which appeared to be directed by sensory clues sensitive to the Earth’s magnetic field. They suggest that the garden warblers migrating from Northern Scandinavia to Southern Africa every year are directed from their detection of the Earth’s magnetic field. They have an internal Sat-Nav. This has been shown in birds such as European Robins and also more recently it was found in domestic chickens, but also turtles and spiny lobsters [59]. The original tests simply placed the birds (European robins) in cages with no sky view, within which they would scratch at the South-Westerly direction, the direction they would be migrating if free. The concept of magnetodetection was deduced from the main finding that when the birds were exposed to an external magnetic field that interfered with the inclination (angle) of the Earth’s magnetic field, they become lost and scratch at all directions. Further, when their eyes are completely covered they become similarly disorientated, suggesting the process is photoinitiated. Not only is the process light-dependent, but magnetodetection in European Robins has shown to be wavelength dependent, see figure 14, [60].

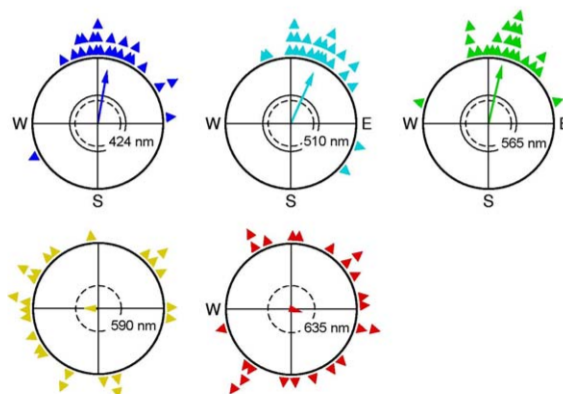


Figure 14. Experiments show birds exposed to monochromatic light exhibit differing orientation behavior- orientation is better in 'bluer' light, from [60].

As explanation there are two dominant theories currently in the field; one essentially is classical; based on ferrimagnetic iron oxide particles in the bird's body. The classical picture describes a magnetically sensitive protein that acts analogously to a physically moving compass. A navigational 'Magnetoreceptor' of this kind has recently been discovered [61]. However for the purposes of this review, we concentrate on the alternative hypothesis which conjectures quantum processes in photoinitiated radical reactions: a Radical Pair Mechanism (RPM). The RPM was first introduced by Schulten [62] and developed further by Ritz [63, 64, 65, 66, 67], his idea that the "chemical compass" in the bird is a light initiated radical pair mechanism, where a disruption to the pair recombination due to magnetic field effects results in interpretation and recognition in the birds nervous system. A proposed such RPM can be described as in figure 15, [68].

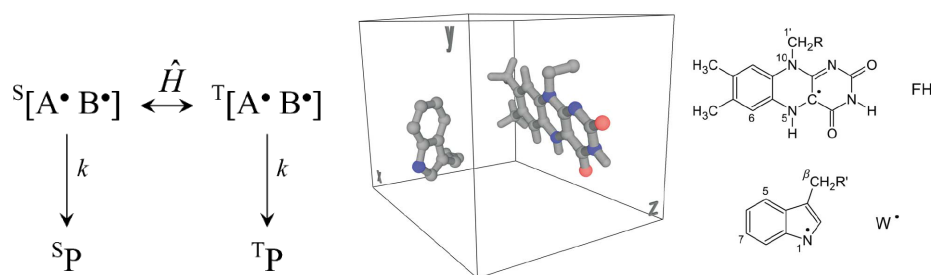
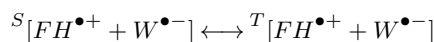


Figure 15. RPM mechanism adapted from [68]. The left shows the photo-initiated radical pair AB (FH and W here), the spin Hamiltonian \hat{H} interconverts the pair from singlet to triplet states, with differing resulting singlet or triplet products as a consequence of the entanglement. in the middle: structures in the box show the tryptophan radical (W) and the flavin radical (FH) at the proposed orientation in vivo, (the possible AB pair). On the left are the 2D structure's for FH and W. The orientation of this possible RP (from pdb code 1DNP) was used to calculate anisotropic magnetic field effects in [68].

Light first excites the donor (D) and acceptor (A) molecules from the electronic ground state, causing electron transfer from $D \rightarrow A$, resulting in unpaired electrons on each: radical pairs.

$$FH + \hbar\omega \rightarrow FH^* \rightarrow [FH^{\bullet+} + W^{\bullet-}] \tag{5.1}$$



It is proposed, see figure 15, that the donor and acceptor may be FH and W respectively, as in 5.1. The radical pairs are initially singlet states (anti-parallel electron spins) but an interaction due to hyperfine coupling leads to conversion into triplet states (parallel electron spins). This singlet-triplet mixing (S-T) is a coherent oscillation of the total electron spin state, determined by the hyperfine constant (which arises due to the interaction between the spin states and the magnetic nuclei in the environment) but also the Zeeman interaction with the external magnetic field B . The rate of this transition back to a recombination of singlet states depends on the orientation of the (Earth's) magnetic field [6] and the interconversion is coherent oscillatory: another quantum beat! For more detail of the coherent oscillations, Kominis [69], shows that different approaches to solve equation 4.9 versus the full QME, can be used to show the time evolution of coherent states $\langle Q_S \rangle_T$. What is interesting to calculate are the rates respectively of k_T triplet product formation versus k_S singlet product formation since this encodes information about the magnetic field. What are the rates for product S_P or S_T formation based on S/T populations?

For this problem, the QME, c.f., equation 4.10, is given by the Haberkorn approach [6]:

$$\frac{\partial \rho}{\partial t} = \frac{-i}{\hbar} [H, \rho] - k_S(Q_S \rho + \rho Q_S) - k_T(Q_T \rho + \rho Q_T), \quad (5.2)$$

where Q_T projects on the triplet subspace and similarly for the singlet subspace. The Hamiltonian of the radical pair in the protein (nuclear) environment is the sum of the hyperfine coupling (left term) and the Zeeman contribution (right term)[6]:

$$H = \sum_{i=D,A} \sum_j s_i T_{ij} I_{ij} - g \mu_B B (\vec{s}_A - \vec{s}_D), \quad (5.3)$$

which introduces the effect of the earth's magnetic field B as discussed above. The Hamiltonian of the radical-pair interaction is given by I_{ij} and s_i which are nuclear and electron spin operators and T_{ij} which is the hyperfine coupling tensor. g is the gyromagnetic ratio and μ_0 is the Bohr magneton, and B the external magnetic field, the strength and direction of which defines the population of triplet versus singlet states. It is found that the longer lived the pair the more sensitive to B the system[68]; if the magnetic Hamiltonian has no time to mix the electron spin, all reaction products will remain singlet. The singlet yield is then determined from [6]:

$$\Phi_S = k_S \int_0^\infty \text{tr}[\rho(t) Q_S] dt. \quad (5.4)$$

The orientation information is derived from the anisotropic hyperfine interaction; the interconversion of $S \leftrightarrow T$ states is dependent on the RP (fixed in a protein in the birds anatomy) relative to the direction of the magnetic field. The hyperfine interactions are anisotropic, so that $k_S \neq k_T$ depending on the orientation of the chromophoric molecules with respect to the field, see figure 15, which shows the variation of Φ_S with respect to orientation (angles Phi and Theta) of the RP at $B = 50 \mu T$ and $k_S = 2 \times 10^5 s^{-1}$ (European Robins magneto-detect within 43 - 54 μT [68]). The changes in rate according to the orientation dependence suggest that the bird responds somehow to the information of the earth's field with respect to these D/A molecules in its anatomy (in its head movement).

(a) Challenges and future prospects

Though the theory is fascinating, an analogous reaction mechanism is shown, see figure 17, it is unknown where anatomically the RPM takes place. The proof of principle is shown, in the case of a synthetic triad of carotenoid (C)- porphyrin (P)-fullerene molecules, [70] that RPs do indeed encode magnetic fields through S/T reaction rates. However this is a synthetic construct and experimental verification and identification of the biological system that may host in actuality this mechanism in animals has not yet been determined. There are various suggestions as to which

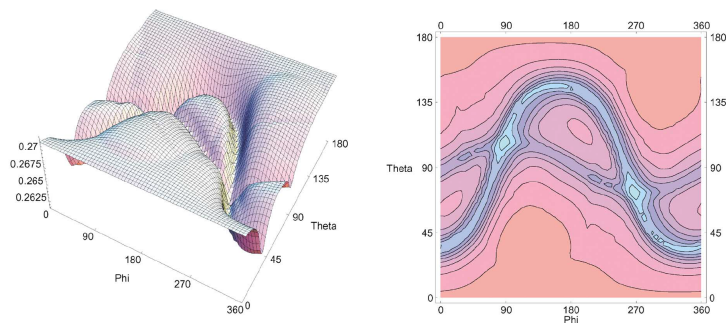


Figure 16. Shows the orientation dependence of the singlet recombination probability Φ_S of the radical pair $[FH^{\bullet+} + W^{\bullet-}]$ as in figure 15, from [68]. Results are for a weak field of $B = 50\mu T$ and $k_S = 2 \times 10^5 s^{-1}$.

protein is responsible, and cryptochrome is the popular contender [71], but this is not certain, and certainly exactly which molecules are the donor and acceptors in the RP is not ascertained either. Figure 15 for example, is based on a D/A pair FH and W which is modelled on FADH and Trp-306 in the E. coli DNA photolyase. This photolyase repairs UV damage to DNA and involves electron transfer, energy transfer and enzymatic processes (all of the above!) but it is not clear this is the protein used in animals for magnetodetection (it is a model construct like figure 17). The RPM is also known to occur in photosynthetic reaction centres, and has been probed with EPR -zero quantum coherences and quantum beats have been observed [72]. Further if the protein conjectured to house the RPM is cryptochrome (which has not been established via EPR and ENDOR experiments to show spin-correlated radical pairs of certain lifetimes) it is still not known how the field information is then passed on to the bird's response. Similar to the limitations in section 3, more needs to be known about the receptor structure responsible, and the possible D/A candidates, especially as in this case, it has been seen that there is an orientation dependence, but also how is the singlet recombination rate then transduced to the bird's nervous system?

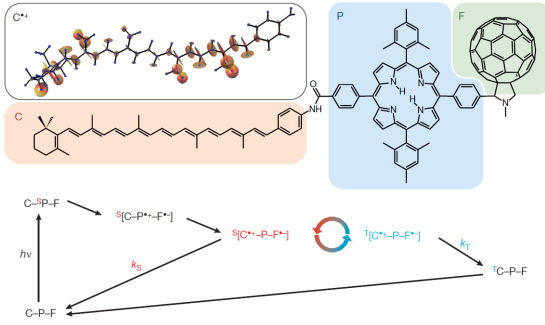


Figure 17. Reaction mechanism (bottom) and 2D structures of the carotenoid (C)- porphyrin (P)-fullerene (F) system (top) that demonstrates the “chemical compass” principle, from [73]. Interconversion between singlet and triplet pair is shown $[C^{\bullet+} - P - F^{\bullet-}]$ as moderated by weak magnetic fields. The rates at which they recombine to C-P-F is spin-selective accounting for rates k_S and k_T . $C^{\bullet+}$ shows the anisotropic hyperfine couplings calculated on C.

6. Conclusions

Four systems have been discussed. All describe rates with differing degrees of possible “quantum effects” hosted in a type of PPC. These quantum effects range from tunneling, as observed in enzyme processes and conjectured in olfaction, to the observations of superpositioned states and persistent coherences in photosynthesis, and finally to entanglement: Einstein’s “spooky action at a distance” in a possible mechanism for magneto-detection in animals. Arguably one of the most astonishing, and common, inference from this examination is counterintuitively, that the environment (the protein) in the PPC does not hinder any of these processes, but actually that it may help.

(a) Environment helps

This review particularly focuses on an environment modelled using normal modes (bosonic baths), though spin baths are touched on in 5. This assumes anharmonic, large amplitude, and long timescale motions are on irrelevant timescales (with respect to the rates described here). If it were otherwise any quantum superposition state carrying information would collapse. It is found, that actually *normal mode* vibrations at least, do not decohere, but rather support and/or accelerate rates. In section 2 Enzymes, the possibility of tunneling being “stabilized by phonon emission” is first introduced. In section 3 Olfaction, tunneling is conjectured to be *assisted* by phonon emission by an odorant. In both it is possible that a vibrational mode may *accept* and/or *promote* the rate. Of course there may also be “demoting” modes. In section 4 Photosynthesis, depending on the coupling regime appropriate, it is found similarly that collective modes may cause environment assisted or dephasing assisted quantum transport. Implementing a Lindblad operator for dephasing also does not necessarily involve decoherence, in photosynthesis see [45], or in olfaction see [33], but supports coherence. It is less obvious that vibrational modes may be useful in magnetoreception, however it has been experimentally shown that the environment does not disguise any effect [73], and it is likely that the D/A pair that encode the field are held at relative orientations optimal for the effect transduction, see figure 15, which is of course determined by the host protein. As is the nuclear environment (the nuclear spin) which is key to coupling to the D/A states, see equation 15, for the asymmetry in reaction rates.

Intriguingly, although protein environments (e.g., enzymes) are more often thought of as insulating barriers (see figure 2 for example) and as “wet and noisy” environments thought not to be any way conducive to the survival of any “quantum effect”, it has been seen that protein motion may serve to promote key quantized events such as charge and energy transfer. Typically proteins can facilitate transfer by: i) reducing the effective tunneling mass by solvent exclusion, ii) enabling crossing by equalization of energy states reactants and products (i.e. moving the Born-Oppenheimer surfaces closer together, see figure 1) iii) and by reducing barrier widths. Note, that the notion that the environment aids a transition does not necessarily imply that the transition is quantum. Perhaps most exciting is the idea that protein motion may support the persistence of coherent oscillations, seen in figure 13, for example at ambient temperatures. Not only support, but that the protein may provide non-classical oscillations that assist the transfer of charge and/or energy [74]. The vast and exciting work done in this area of photosynthesis is indubitably aided and fueled by the advancement in experimental evidence, see section (a), that definitively shows a quantum phenomena, and highlights a need for future work in the other areas.

(b) Challenges in general and future outlook

As mentioned above, it is clear the field of “quantum effects in biology” is most well tested in photosynthesis - where quantum processes have been directly observed. Structures of photosynthetic apparatus provide more reliable information on the relevant states involved. This is not true exactly for magnetodetection and olfaction for example. The analysis can only be as good as the representative Hamiltonian, which defines all interactions and forces driving the

system, and not knowing the likely D/A states, let alone with the precision required, is a huge bottleneck in these fields. Designing experiments, then, that directly test hypothesizes here, at the quantum level, must thus be a priority for advancement. Until then, though interesting, quantum effects remain conjecture, and any analysis is really redundant without experimental proof. It is hoped however, that the theory and some concepts mentioned here highlight promise, and that the developments will continue. In these fields and beyond, there is still much more to discuss, neglected here is work in quantum computing, or quantum simulators as in Mostame et al [75], where biological mimetics may suggest promise. In fact “quantum effects” and the exploration thereof have indicated to be useful in various fields: DNA mutations [76], vision [77], and even consciousness [78], to name a few, all of which may also exhibit surprising quantum effects and provide fascinating avenues for future examination.

Acknowledgements. This work has benefitted enormously by input from Gavin Vinson, Dorothy Duffy, Joonsuk Huh, JohnJoe McFadden and Alex Connor, much gratitude to them for their time and assistance. With thanks also to the support I have received from Marshall Stoneham, Andrew Fisher and Rachel McKendry.

References

- 1 Klinman JP, Kohen A. Hydrogen tunneling links protein dynamics to enzyme catalysis. *Annual review of biochemistry*. 2013 jan;82:471–96. Available from: <http://www.annualreviews.org/doi/abs/10.1146/annurev-biochem-051710-133623>.
- 2 DeVault D. *Quantum-Mechanical Tunneling in Biological Systems*. vol. 2nd. Cambridge University Press; 1984.
- 3 Eyring H. The Activated Complex and the Absolute Rate of Chemical Reactions. *Chemical Reviews*. 1935 aug;17(1):65–77. Available from: <http://dx.doi.org/10.1021/cr60056a006>.
- 4 Gray HB, Winkler JR. Long-range electron transfer. *Proceedings of the National Academy of Sciences of the United States of America*. 2005;102(10):3534–3539.
- 5 Oppenheimer JR. Three Notes on the Quantum Theory of Aperiodic Effects. *Physical Review*. 1928 jan;31(1):66–81. Available from: <http://link.aps.org/doi/10.1103/PhysRev.31.66>.
- 6 Huelga SF, Plenio MB. Vibrations, Quanta and Biology. *Contemporary Physics*. 2013;54(27 June):181–207. Available from: <http://arxiv.org/abs/1307.3530>.
- 7 Pauling L. Chemical achievement and hope for the future. *American scientist*. 1948 jan;36(1):51–8. Available from: <https://www.ncbi.nlm.nih.gov/pubmed/18920436>.
- 8 DeVault D, Chance B. Studies of photosynthesis using a pulsed laser. I. Temperature dependence of cytochrome oxidation rate in chromatium. Evidence for tunneling. *Biophysical journal*. 1966 nov;6(6):825–47. Available from: <https://www.ncbi.nlm.nih.gov/pubmed/5972381>.
- 9 Hay S, Scrutton NS. Good vibrations in enzyme-catalysed reactions. *Nature Chemistry*. 2012;4(3):161–168. Available from: <http://dx.doi.org/10.1038/nchem.1223>.
- 10 Grant KL, Klinman JP. Evidence that both protium and deuterium undergo significant tunneling in the reaction catalyzed by bovine serum amine oxidase. *Biochemistry*. 1989 aug;28(16):6597–6605. Available from: <http://dx.doi.org/10.1021/bi00442a010>.
- 11 Bendall DS. *Protein Electron Transfer*. BIOS Scientific Publishers; 1996.
- 12 Hopfield JJ. Kinetic Proofreading: A New Mechanism for Reducing Errors in Biosynthetic Processes Requiring High Specificity. *Proceedings of the National Academy of Sciences*. 1974 oct;71(10):4135–4139. Available from: <http://www.pnas.org/content/71/10/4135.short>.
- 13 Huang K, Rhys A. Theory of Light Absorption and Non-Radiative Transitions in F-Centres. *Proceedings of the Royal Society A: Mathematical, Physical and Engineering Sciences*. 1950 dec;204(1078):406–423. Available from: <http://rspa.royalsocietypublishing.org/content/204/1078/406>.

- 14 Jortner J, Ben-Reuven A. Intermolecular electronic energy transfer induced by an intense optical radiation field. *Chemical Physics Letters*. 1976 aug;41(3):401–406. Available from: <http://www.sciencedirect.com/science/article/pii/0009261476853821>.
- 15 Pudney CR, Lane RSK, Fielding AJ, Magennis SW, Hay S, Scrutton NS. Enzymatic single-molecule kinetic isotope effects. *Journal of the American Chemical Society*. 2013 mar;135(10):3855–3864. Available from: <http://dx.doi.org/10.1021/ja309286r>.
- 16 Kandathil SM, Driscoll MD, Dunn RV, Scrutton NS, Hay S. Proton tunnelling and promoting vibrations during the oxidation of ascorbate by ferricyanide? *Physical chemistry chemical physics : PCCP*. 2014;16(6):2256–2259. Available from: <http://pubs.rsc.org/en/content/articlehtml/2014/cp/c3cp55131h>.
- 17 Hay S, Scrutton NS. Good vibrations in enzyme-catalysed reactions. *Nature chemistry*. 2012 mar;4(3):161–168. Available from: <http://dx.doi.org/10.1038/nchem.1223>.
- 18 Vlček A, Kvapilová H, Towrie M, Zálíš S. Electron-Transfer Acceleration Investigated by Time Resolved Infrared Spectroscopy. *Accounts of Chemical Research*. 2015;p. 150220103925008. Available from: <http://pubs.acs.org/doi/abs/10.1021/ar5004048>.
- 19 Vinh NQ, Redlich B, van der Meer AFG, Pidgeon CR, Greenland PT, Lynch SA, et al. Time-Resolved Dynamics of Shallow Acceptor Transitions in Silicon. *Physical Review X*. 2013 mar;3(1):011019. Available from: <http://link.aps.org/doi/10.1103/PhysRevX.3.011019>.
- 20 Buck L. A novel multigene family may encode odorant receptors: A molecular basis for odor recognition. *Cell*. 1991;65(1):175–187. Available from: <http://www.cell.com/retrieve/pii/009286749190418X>.
- 21 Sell CS. On the unpredictability of odor. *Angewandte Chemie (International ed in English)*. 2006 sep;45(38):6254–61. Available from: <http://www.ncbi.nlm.nih.gov/pubmed/16983730>.
- 22 Tobar HF, Moreno PA, Vélez PE. Highly conserved regions in the 5' region of human olfactory receptor genes. *Genetics and Molecular Research: GMR*. 2009;8(1):117–128. Available from: <http://www.ncbi.nlm.nih.gov/pubmed/19283679>.
- 23 Harini K, Sowdhamini R. Computational Approaches for Decoding Select Odorant-Olfactory Receptor Interactions Using Mini-Virtual Screening. *PloS one*. 2015 jan;10(7):e0131077. Available from: <http://journals.plos.org/plosone/article?id=10.1371/journal.pone.0131077>.
- 24 Salom D, Lodowski DT, Stenkamp RE, Le Trong I, Golczak M, Jastrzebska B, et al. Crystal structure of a photoactivated deprotonated intermediate of rhodopsin. *Proceedings of the National Academy of Sciences*. 2006 oct;103(44):16123–16128. Available from: <https://www.ncbi.nlm.nih.gov/pubmed/17060607>.
- 25 Malcolm Dyson G. The scientific basis of odour. *Journal of the Society of Chemical Industry*. 1938 jul;57(28):647–651. Available from: <http://doi.wiley.com/10.1002/jctb.5000572802>.
- 26 Wright RHH. Odor and molecular vibration: Neural coding of olfactory information. *Journal of Theoretical Biology*. 1977 feb;64(3):473–502. Available from: <http://www.sciencedirect.com/science/article/pii/0022519377902831>.
- 27 <http://doi.org/10.1093/chemse/21.6.773> Turin, LucaTurin, L (1996) A Spectroscopic Mechanism for Primary Olfactory Reception *Chemical Senses*, 21(6) â, Turin L. A Spectroscopic Mechanism for Primary Olfactory Reception. *Chemical Senses*. 1996;21(6):773–791. Available from: <http://chemse.oxfordjournals.org/content/21/6/773.abstract>.
- 28 Lambe J, Jaklevic RC. Molecular Vibration Spectra by Inelastic Electron Tunneling. *Physical Review*. 1968;165(3):821–832. Available from: <http://journals.aps.org/pr/abstract/10.1103/PhysRev.165.821>.
- 29 Brookes JC, Hartoutsiou F, Horsfield AP, Stoneham AM. Could Humans Recognize Odor by Phonon Assisted Tunneling? *Physical Review Letters*. 2007;98(3):38101. Available from: <http://journals.aps.org/prl/abstract/10.1103/PhysRevLett.98.038101>.
- 30 Narth C, Gillet N, Cailliez F, Lévy B, de la Lande A. Electron Transfer, Decoherence, and Protein Dynamics: Insights from Atomistic Simulations. *Accounts of Chemical Research*.

- 2015;p. 150302152735001. Available from: <http://pubs.acs.org/doi/abs/10.1021/ar5002796>.
- 31 Brookes JC. Olfaction: the physics of how smell works? *Contemporary Physics*. 2011;52(5):385–402. Available from: <http://www.tandfonline.com/doi/abs/10.1080/00107514.2011.597565?journalCode=tcph20>.
- 32 Solov'yov IA, Chang PY, Schulten K. Vibrationally assisted electron transfer mechanism of olfaction: myth or reality? *Physical chemistry chemical physics : PCCP*. 2012 oct;14(40):13861–71. Available from: <http://pubs.rsc.org/en/Content/ArticleHTML/2012/CP/C2CP41436H>.
- 33 Checinska a, Pollock Fa, Heaney L, Nazir A, Chęcińska A, Pollock Fa, et al. Dissipation enhanced vibrational sensing in an olfactory molecular switch. *arXiv: 14036483*. 2014;142(2):1–12. Available from: <http://arxiv.org/abs/1403.6483>.
- 34 Tirandaz A, Taher Ghahramani F, Shafiee A. Dissipative vibrational model for chiral recognition in olfaction. *Physical Review E*. 2015 sep;92(3):032724. Available from: <http://link.aps.org/doi/10.1103/PhysRevE.92.032724>.
- 35 Takai Y, Touhara K. Enantioselective recognition of menthol by mouse odorant receptors. *Bioscience, biotechnology, and biochemistry*. 2015 dec;79(12):1980–6. Available from: <http://www.tandfonline.com/doi/abs/10.1080/09168451.2015.1069697>.
- 36 Haffenden LJW, Yaylayan Va, Fortin J. Investigation of vibrational theory of olfaction with variously labelled benzaldehydes. *Food Chemistry*. 2001;73(1):67–72.
- 37 Keller A, Vosshall LB. A psychophysical test of the vibration theory of olfaction. *Nature neuroscience*. 2004 apr;7(4):337–8. Available from: <http://dx.doi.org/10.1038/nn1215>.
- 38 Gane S, Georganakis D, Maniati K, Vamvakias M, Ragoussis N, Skoulakis EMC, et al. Molecular Vibration-Sensing Component in Human Olfaction. *PLoS ONE*. 2013;8(1).
- 39 Franco MI, Turin L, Mershin A, Skoulakis EMC. Molecular vibration-sensing component in *Drosophila melanogaster* olfaction. *Proceedings of the National Academy of Sciences*. 2011; Available from: <http://www.pnas.org/content/early/2011/02/08/1012293108.abstract>.
- 40 Gronenberg W, Raikhelkar A, Abshire E, Stevens J, Epstein E, Loyola K, et al. Honeybees (*Apis mellifera*) learn to discriminate the smell of organic compounds from their respective deuterated isotopomers. *Proceedings Biological sciences / The Royal Society*. 2014 mar;281(1778):20133089. Available from: <http://rspb.royalsocietypublishing.org/content/281/1778/20133089>.
- 41 Block E, Jang S, Matsunami H, Sekharan S, Dethier B, Ertem MZ, et al. Implausibility of the vibrational theory of olfaction. *Proceedings of the National Academy of Sciences*. 2015;p. 201503054. Available from: <http://www.pnas.org/lookup/doi/10.1073/pnas.1503054112>.
- 42 Lin SH. Effect of Partial Deuteration and Temperature on Triplet-State Lifetimes. *The Journal of Chemical Physics*. 1968 sep;48(6):2732. Available from: <http://scitation.aip.org/content/aip/journal/jcp/48/6/10.1063/1.1669507>.
- 43 Barwich AS. What is so special about smell? Olfaction as a model system in neurobiology. *Postgraduate medical journal*. 2015 nov;p. postgradmedj–2015–133249–. Available from: <http://pmj.bmj.com/content/early/2015/11/03/postgradmedj-2015-133249.abstract>.
- 44 Hoehn RD, Nichols D, Neven H, Kais S. Neuroreceptor activation by vibration-assisted tunneling. *Scientific reports*. 2015 jan;5:9990. Available from: <http://www.nature.com/srep/2015/150424/srep09990/full/srep09990.html>.
- 45 Mohseni M, Rebentrost P, Lloyd S, Aspuru-Guzik A. Environment-assisted quantum walks in photosynthetic energy transfer. *The Journal of chemical physics*. 2008 nov;129(17):174106. Available from: <http://scitation.aip.org/content/aip/journal/jcp/129/17/10.1063/1.3002335>.
- 46 Hayes D, Wen J, Panitchayangkoon G, Blankenship RE, Engel GS. Robustness of electronic coherence in the Fenna-Matthews-Olson complex to vibronic and structural modifications.

- Faraday Discussions. 2011 jul;150:459. Available from: <http://pubs.rsc.org/en/Content/ArticleHTML/2011/FD/C0FD00030B>.
- 47 Mohseni \hat{A} , Omar \hat{A} , Engel \hat{A} , Plenio \hat{A} . Quantum Effects in Biology. Cambridge University Press; 2014.
- 48 Ishizaki A, Fleming GR. Quantum superpositions in photosynthetic light harvesting: delocalization and entanglement. *New Journal of Physics*. 2010 may;12(5):55004. Available from: <http://iopscience.iop.org/article/10.1088/1367-2630/12/5/055004>.
- 49 Christensson N, Kauffmann HF, Pullerits T, Mančal T. Origin of long-lived coherences in light-harvesting complexes. *Journal of Physical Chemistry B*. 2012 jun;116(25):7449–7454. Available from: <http://dx.doi.org/10.1021/jp304649c>.
- 50 Chenu A, Scholes GD. Coherence in energy transfer and photosynthesis. *Annual review of physical chemistry*. 2015 Apr;66:69–96. Available from: <http://www.annualreviews.org/doi/abs/10.1146/annurev-physchem-040214-121713>.
- 51 Engel GS, Calhoun TR, Read EL, Ahn TK, Mancal T, Cheng YC, et al. Evidence for wavelike energy transfer through quantum coherence in photosynthetic systems. *Nature*. 2007 apr;446(7137):782–6. Available from: <http://dx.doi.org/10.1038/nature05678>.
- 52 Roden JJJ, Bennett DIG, Whaley KB. Long-range energy transport in photosystem II. *Journal of Chemical Physics*. 2016 jun;144(24):245101. Available from: <http://scitation.aip.org/content/aip/journal/jcp/144/24/10.1063/1.4953243>.
- 53 Allegra M, Giorda P, Lloyd S. Global coherence of quantum evolutions based on decoherent histories: theory and application to photosynthetic quantum energy transport. 2015;p. 1–25. Available from: <http://arxiv.org/abs/1503.04735>.
- 54 Shim S, Rebentrost P, Valleau S, Aspuru-Guzik A. Atomistic Study of the Long-Lived Quantum Coherences in the Fenna-Matthews-Olson Complex. *Biophysical Journal*. 2012;102(3):649–660. Available from: [http://www.cell.com/biophysj/abstract/S0006-3495\(11\)05423-3](http://www.cell.com/biophysj/abstract/S0006-3495(11)05423-3).
- 55 Lindblad G. Brownian motion of a quantum harmonic oscillator. *Reports on Mathematical Physics*. 1976 dec;10(3):393–406. Available from: <http://www.sciencedirect.com/science/article/pii/003448777690029X>.
- 56 Jeske J, Ing DJ, Plenio MB, Huelga SF, Cole JH. Bloch-Redfield equations for modeling light-harvesting complexes. *The Journal of chemical physics*. 2015 Feb;142(6):064104. Available from: <http://scitation.aip.org/content/aip/journal/jcp/142/6/10.1063/1.4907370>.
- 57 Panitchayangkoon G, Hayes D, Fransted KA, Caram JR, Harel E, Wen J, et al. Long-lived quantum coherence in photosynthetic complexes at physiological temperature. *Proceedings of the National Academy of Sciences of the United States of America*. 2010 jul;107(29):12766–12770. Available from: <http://www.pnas.org/content/107/29/12766.abstract>.
- 58 Adolphs J, Renger T. How Proteins Trigger Excitation Energy Transfer in the FMO Complex of Green Sulfur Bacteria. *Biophysical Journal*. 2006;91(8):2778–2797. Available from: <http://www.sciencedirect.com/science/article/pii/S0006349506719932internal-pdf://1203/S0006349506719932.html>.
- 59 Wiltschko W, Wiltschko R. Magnetic orientation and magnetoreception in birds and other animals. *Journal of comparative physiology A, Neuroethology, sensory, neural, and behavioral physiology*. 2005;191(8):675–693. Available from: <http://www.ncbi.nlm.nih.gov/pubmed/15886990>.
- 60 Wolfgang Wiltschko RW, Wiltschko W, Wiltschko R. Magnetoreception in birds: two receptors for two different tasks. *Journal of Ornithology*. 2007;148:61–76. Available from: <http://link.springer.com/article/10.1007/s10336-007-0233-2>.
- 61 Qin S, Yin H, Yang C, Dou Y, Liu Z, Zhang P, et al. A magnetic protein biocompass. *Nature Materials*. 2015 nov;advance on. Available from: <http://dx.doi.org/10.1038/nmat4484>.
- 62 Ritz T, Adem S, Schulten K. A model for photoreceptor-based magnetoreception in birds. *Biophysical journal*. 2000 feb;78(2):707–18. Available from: <https://www.ncbi.nlm.nih.gov/pmc/articles/PMC1300674/>.

- 63 Ritz T, Thalau P, Phillips JB, Wiltschko R, Wiltschko W. Resonance effects indicate a radical-pair mechanism for avian magnetic compass. *Nature*. 2004 may;429(6988):177–80. Available from: <http://dx.doi.org/10.1038/nature02534>.
- 64 Ritz T, Wiltschko R, Hore PJ, Rodgers CT, Stapput K, Thalau P, et al. Magnetic compass of birds is based on a molecule with optimal directional sensitivity. *Biophysical journal*. 2009 apr;96(8):3451–3457. Available from: <http://www.sciencedirect.com/science/article/pii/S0006349509004688>.
- 65 Ritz T. Quantum effects in biology: Bird navigation. *Procedia Chemistry*. 2011;3(1):262–275. Available from: <http://www.sciencedirect.com/science/article/pii/S1876619611000738>.
- 66 Wang K, Mattern E, Ritz T. On the use of magnets to disrupt the physiological compass of birds. *Physical biology*. 2006;3(3):220–231.
- 67 Wiltschko R, Thalau P, Gehring D, Niefner C, Ritz T, Wiltschko W. Magnetoreception in birds: the effect of radio-frequency fields. *Journal of the Royal Society, Interface / the Royal Society*. 2015 feb;12(103):20141103–. Available from: <http://rsif.royalsocietypublishing.org/content/12/103/20141103.abstract>.
- 68 Cintolesi F, Ritz T, Kay CWM, Timmel CR, Hore PJ. Anisotropic recombination of an immobilized photoinduced radical pair in a 50-uT magnetic field: A model avian photomagnetoceptor. *Chemical Physics*. 2003;294(3):385–399.
- 69 Kominis IK. Magnetic sensitivity and entanglement dynamics of the chemical compass. *Chemical Physics Letters*. 2012;542:143–146. Available from: <http://dx.doi.org/10.1016/j.cplett.2012.06.014>.
- 70 Maeda K, Henbest KB, Cintolesi F, Kuprov I, Rodgers CT, Liddell PA, et al. Chemical compass model of avian magnetoreception. *Nature*. 2008;453(7193):387–390. Available from: <http://www.readcube.com/articles/10.1038/nature06834internal-pdf://1139/nature06834.html>.
- 71 Foley LE, Gegear RJ, Reppert SM. Human cryptochrome exhibits light-dependent magnetosensitivity. *Nature communications*. 2011;2(May):356. Available from: <http://dx.doi.org/10.1038/ncomms1364>.
- 72 Bittl R, Kothe G. Transient EPR of radical pairs in photosynthetic reaction centers: prediction of quantum beats. *Chemical Physics Letters*. 1991 Mar;177(6):547–553. Available from: <http://www.sciencedirect.com/science/article/pii/000926149190082K>.
- 73 Maeda K, Liddell P, Gust D, Hore PJ. Spin-selective recombination reactions of radical pairs: experimental test of validity of reaction operators. *The Journal of chemical physics*. 2013 dec;139(23):234309. Available from: <http://scitation.aip.org/content/aip/journal/jcp/139/23/10.1063/1.4844355>.
- 74 O'Reilly EJ, Olaya-Castro A. Non-classicality of the molecular vibrations assisting exciton energy transfer at room temperature. *Nature communications*. 2014;5:3012. Available from: <https://www.ncbi.nlm.nih.gov/pubmed/24402469>.
- 75 Mostame S, Rebentrost P, Eisfeld A, Kerman AJ, Tsomokos DI, Aspuru-Guzik A. Quantum simulator of an open quantum system using superconducting qubits: Exciton transport in photosynthetic complexes. *New Journal of Physics*. 2012 oct;14(10):0–21. Available from: <http://stacks.iop.org/1367-2630/14/i=10/a=105013>.
- 76 McFadden J, Al-Khalili J. A quantum mechanical model of adaptive mutation. *Biosystems*. 1999 jun;50(3):203–211. Available from: <http://www.sciencedirect.com/science/article/pii/S0303264799000040>.
- 77 Kukura P, McCamant DW, Yoon S, Wandschneider DB, Mathies RA. Structural Observation of the Primary Isomerization in Vision with Femtosecond-Stimulated Raman. *Science*. 2005;310(5750):1006–1009. Available from: <https://www.ncbi.nlm.nih.gov/pubmed/16284176>.
- 78 Romero-Isart O, Juan ML, Quidant R, Cirac JJ, et Al AM, S HKSASPE, et al. Toward quantum superposition of living organisms. *New Journal of Physics*. 2010 mar;12(3):033015. Available from: <http://stacks.iop.org/1367-2630/12/i=3/a=033015?key=crossref.72857b9122ea9b36ccf9f2b1c9d6f505>.